

Human Protein-L-isoaspartate O-Methyltransferase Domain-Containing Protein 1 (PCMTD1) Associates with Cullin-RING Ligase Proteins

Rebecca A. Warmack,[†] Eric Z. Pang,[†] Esther Peluso, Jonathan D. Lowenson, Joseph Y. Ong, Jorge Z. Torres, and Steven G. Clarke^{*}



Cite This: *Biochemistry* 2022, 61, 879–894



Read Online

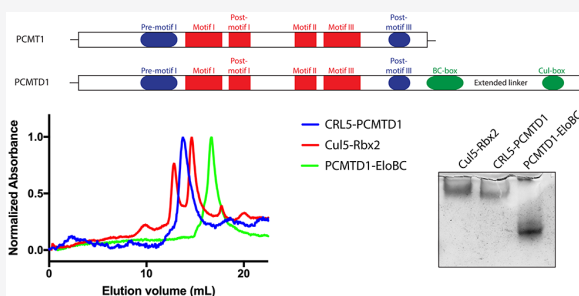
ACCESS |

Metrics & More

Article Recommendations

Supporting Information

ABSTRACT: The spontaneous L-isoaspartate protein modification has been observed to negatively affect protein function. However, this modification can be reversed in many proteins in reactions initiated by the protein-L-isoaspartyl (D-aspartyl) O-methyltransferase (PCMT1). It has been hypothesized that an additional mechanism exists in which L-isoaspartate-damaged proteins are recognized and proteolytically degraded. Herein, we describe the protein-L-isoaspartate O-methyltransferase domain-containing protein 1 (PCMTD1) as a putative E3 ubiquitin ligase substrate adaptor protein. The N-terminal domain of PCMTD1 contains L-isoaspartate and S-adenosylmethionine (AdoMet) binding motifs similar to those in PCMT1. This protein also has a C-terminal domain containing suppressor of cytokine signaling (SOCS) box ubiquitin ligase recruitment motifs found in substrate receptor proteins of the Cullin-RING E3 ubiquitin ligases. We demonstrate specific PCMTD1 binding to the canonical methyltransferase cofactor S-adenosylmethionine (AdoMet). Strikingly, while PCMTD1 is able to bind AdoMet, it does not demonstrate any L-isoaspartyl methyltransferase activity under the conditions tested here. However, this protein is able to associate with the Cullin-RING proteins Elongins B and C and Cul5 *in vitro* and in human cells. The previously uncharacterized PCMTD1 protein may therefore provide an alternate maintenance pathway for modified proteins in mammalian cells by acting as an E3 ubiquitin ligase adaptor protein.



INTRODUCTION

Proteins can accumulate a number of nonenzymatic post-translational modifications over time that alter the normal enzymatic function and threaten protein stability. These modifications include oxidation, carbonylation, glycation, deamidation, and isomerization, which can occur by inter- or intramolecular reactions.¹ Despite this variety of damaging alterations, few protein repair mechanisms have been characterized. Examples of protein repair pathways include methionine sulfoxide reductases, protein deglycation, and L-isoaspartate methylation.^{2–4} The latter is accomplished *via* the protein-L-isoaspartyl (D-aspartyl) O-methyltransferase (PCMT1) enzyme. By methylating L-isoaspartate and D-aspartate sites, PCMT1 allows for subsequent reformation of L-aspartate.⁴

In parallel, many modified proteins are funneled to the lysosome or the proteasome in mammalian cells for degradation.⁵ While the lysosome is a powerful protein degradation system capable of breaking down whole aggregates, organelles, and aged cytosolic proteins, proteasomal degradation is highly regulated and is monitored by the ubiquitin–proteasome system. The latter system involves over

600 E3 ubiquitin ligases in eukaryotic cells where targeted substrates are recognized.^{6,7} Among the E3 ubiquitin ligases, the Cullin-RING ligase (CRL) family is the largest subset.⁸ These E3 ubiquitin ligases contain conserved RING domains that recruit Cullin scaffold proteins. Full complex formation positions an E2 enzyme opposite bound substrates for ubiquitin transfer.⁹

The Elongin–Cullin–suppressor of cytokine signaling (SOCS) box family is a subgroup of the RING ligase family.¹⁰ This group is characterized by the presence of a SOCS box motif found in the C-terminus of the complex’s substrate adaptor protein (the SOCS box-containing protein).¹⁰ This motif consists of both a Cul-box and a BC-box, which facilitate interactions with Cullin 5 (Cul5), and the heterodimer adaptor

Received: March 7, 2022

Revised: April 15, 2022

Published: April 29, 2022



Table 1. Bacterial Expression Plasmids Used in This Study

plasmid	description	marker	source or reference
pET28a+–rhPCMT	pET28a(+) vector expressing N-terminally 6xHis-tagged human PCMT sequence	Kan ^r	gift from Dr. Bruce Downie (Addgene catalog # 34852)
pMAPLe4–PCMTD1	pMAPLe4 vector expressing full-length N-terminally 6xHis-tagged human PCMTD1 sequence (residues 1–357)	Kan ^r	this study
pMAPLe4–PCMTD1 ^{1–231}	pMAPLe4 vector expressing truncated N-terminally 6xHis-tagged human PCMTD1 sequence (residues 1–231)	Kan ^r	this study
ELONGIN BC (XX01TCEB1A-c001)	Elongin B and Elongin C coexpression plasmids; full-length human Elongin B and amino acids 17–112 of human Elongin C	Clm ^r	Addgene (catalog # 110274)
pET28a_Cul5	pET28a vector expressing Cul5 with an N-terminal 6xHis-tag, GB1 tag, and TEV cleavage site (6xHis–GB1–TEV–Cul5)	Kan ^r	gift from Dr. Elizabeth Komives
pET11a_Rbx2	pET11a vector expressing untagged Rbx2	Amp ^r	gift from Dr. Elizabeth Komives

proteins Elongins B and C, respectively. The SOCS box-containing E3 ligase adaptor protein and the Elongins interact with the N-terminus of the Cul5 scaffold protein, while the C-terminal domain of Cul5 binds Rbx1 or Rbx2 for recruitment of an activated E2 ligase. The open-ring structure of this complex allows coordination between a substrate (recruited to this complex by the SOCS box-containing E3 ligase) to an activated E2 ligase bound to the tail end of the complex. This allows for ubiquitin transfer to a lysine on the surface of the substrate protein.¹¹

A degradation pathway for L-isoaspartate-damaged proteins was proposed when levels of L-isoaspartate residues in proteins unexpectedly plateaued with respect to age in tissues yet appeared in urinary peptides of transgenic mice lacking the L-isoaspartate repair enzyme, PCMT1, in all cell types except neurons.¹² In this work, we describe a potential pathway for such degradation with the initial characterization of protein-L-isoaspartate O-methyltransferase domain-containing protein 1 (PCMTD1).¹³ At its N-terminus, PCMTD1 contains L-isoaspartate and S-adenosylmethionine (AdoMet) binding motifs comparable to the PCMT1 enzyme. The protein also contains an extended SOCS box motif within its C-terminus. Previous reports have linked mutations or deletions of the PCMTD1 and PCMTD2 genes to neurodevelopmental disorders,^{14,15} viral activation,¹⁶ and cancer.¹⁷ Thus, the biochemical characterization of these poorly understood proteins may be of clinical importance.

Using recombinantly expressed constructs, we show that the human PCMTD1 protein interacts with Elongins B and C and Cul5. We observe that the interaction with Elongins B and C appears to stabilize recombinantly expressed PCMTD1 protein levels. Furthermore, using a truncated variant of PCMTD1, the C-terminal SOCS box motif has been found essential for Cul5 and Elongin B and C interactions. While the PCMTD1 enzyme binds the methyltransferase cofactor AdoMet, it has no detectable methyltransferase activity when tested against canonical PCMT1 L-isoaspartate-containing substrates *in vitro*. Lastly, we observe interactions between recombinantly purified preparations of PCMTD1–EloBC and Cul5–Rbx2 subcomplexes, which suggests that these proteins oligomerize into a larger protein complex reminiscent of other Cullin-RING E3 ligases. Although specific substrates have yet to be identified, the PCMTD1 protein may represent a novel protein damage-specific E3 ubiquitin ligase when complexed with components of the Cullin-RING E3 ligase.

■ EXPERIMENTAL PROCEDURES

Reagents and Plasmids. Full-length (1–357) and truncated (1–231) PCMTD1 were expressed as N-terminal

6xHis-tagged constructs in pMAPLe4 vectors designed and generated in the UCLA DOE Protein Expression Technology Core. The vector includes a pBR322 origin and lacI gene. Transgenes in this vector are expressed as an N-terminal MBP–TVMV–6xHis fusion protein. This vector also coexpresses the TVMV protease, which allows for intracellular processing of the fusion protein transgene yielding a target protein with a TEV-cleavable N-terminal 6xHis-tag. Elongins were expressed on the ELONGIN BC plasmid (XX01TCEB1A-c001), which was a gift from Dr. Nicola Burgess-Brown (Addgene plasmid #110274). The plasmid encoding the recombinant human L-isoaspartyl protein methyltransferase (rhPIMT) with an N-terminal polyhistidine tag was a generous gift from Dr. Bruce Downie (available as plasmid #34852 from Addgene). Plasmids for the recombinant expression of 6xHis–GB1–TEV–Cul5 (pET28a_Cul5) and untagged Rbx2 (pET11a_Rbx2) were generous gifts from Dr. Elizabeth Komives. pGLAP2 plasmids (Addgene plasmid #19703) for PCMTD1 and enhanced green fluorescent protein (EGFP) were constructed from their respective pDONR221 plasmids using LR Clonase II (Invitrogen, catalog #11791020) with standard cloning techniques.

Protein BLAST, Sequence Identification and Alignment, and Phylogenetic Analyses. For PCMTD1 sequence alignment and subsequent phylogenetic analyses, an NCBI protein BLAST search was first performed.¹⁸ The protein sequence for PCMTD1 isoform 1 was used as a query against the nonredundant protein sequence (nr) database with nonredundant RefSeq proteins (WP) excluded. The blastp (protein–protein BLAST) algorithm was used. The maximum number of target sequences selected was 5000 with an expected threshold cutoff of 1×10^{-6} . All other parameters were left as default. This search yielded 4118 sequences. PCMTD1 isoform 1 sequences from organisms were manually selected resulting in a total of 399 sequences selected. These sequences were imported into JALVIEW 2.11.1.0¹⁹ and aligned using the T-Coffee algorithm with default settings unless otherwise noted,²⁰ and sequences were color-coded according to ClustalX rules. T-Coffee alignments were imported into the MEGAX program,²¹ and trees were generated using the phylogeny tool with maximum likelihood methods. Default methods for maximum likelihood analysis were used and are as follows: test of phylogeny (none), substitution model (Jones–Taylor–Thornton (JTT) model), rates among sites (uniform rates), data subset to use (use all sites), ML heuristic method (nearest-neighbor-interchange (NNI)), and branch swap filter (none). Multiple sequence alignment of PCMT with the PCMTDs was done with Clustal Omega²² and UniProt accession numbers P22061-1

(PCMT1), Q96MG8-1 (PCMTD1), and Q9NV79-1 (PCMTD2).

Recombinant Protein Expression and Purification.

Plasmids used for recombinant protein purification are described in Table 1. The PCMTD1–EloBC coexpression strain was created by cotransforming competent BL21(DE3) cells with pMAPLe4–PCMTD1 and ELONGIN BC. The PCMTD1^{1–231} expression strain was created by transforming competent BL21(DE3) cells with pMAPLe–PCMTD1^{1–231}. The PCMTD1^{1–231}–EloBC coexpression strain was created by cotransforming competent *Escherichia coli* BL21(DE3) strains with the pMAPLe–PCMTD1^{1–231} and ELONGIN BC plasmids. The Cul5–Rbx2 coexpression strain was created by sequentially transforming competent BL21(DE3) cells with pET28a_Cul5, pET11a_Rbx2, and ELONGIN BC. All transformants were selected by plating on Luria–Bertani (LB) agar with appropriate antibiotics.

For growth and expression, the PCMTD1–EloBC coexpression strain was grown in LB media and induced with 0.5 mM isopropyl β -D-1-thiogalactopyranoside (IPTG) for 3 h at 37 °C when OD₆₀₀ = 0.5–0.7. The PCMTD1^{1–231} and PCMTD1^{1–231}–EloBC expression strains were also grown in LB media but were instead induced overnight for 16–18 h at 18 °C with 1 mM IPTG. These strains were also induced when OD₆₀₀ = 0.5–0.7. The Cul5–Rbx2 coexpression strain was grown in M9 minimal media supplemented with casein enzymatic hydrolysate (M9-NZ). This strain was induced at an OD₆₀₀ of 1.0 with 0.5 mM IPTG. Just prior to induction, M9-NZ was supplemented with ZnCl₂ to a final concentration of 200 μ M to stabilize Rbx2-containing cultures. Cul5–Rbx2 was induced for 16–18 h at 18 °C.

Following expression, cells for all expression strains were spun down for 15 min at 5000g at 4 °C and frozen at –80 °C until lysis and purification. Thawed cells were resuspended in 5 mL/g pellet of lysis buffer (50 mM N-(2-hydroxyethyl)-piperazine-*N'*-ethanesulfonic acid (HEPES), pH 7.6, 300 mM NaCl, 5% glycerol, 1 mM β -mercaptoethanol (β ME), 1 mM phenylmethylsulfonyl fluoride (PMSF), and 1 ethylenediaminetetraacetic acid (EDTA)-free Pierce protease inhibitor tablet per 50 mL). Lysis was performed by three passes through an Avestin Emulsiflex at 15,000 psi with incubations on ice to minimize the temperatures of lysates. Lysates were then spun at 13,000 rpm for 50 min at 4 °C. Filtered lysates were then loaded onto three 5 mL HisTrap HP columns equilibrated with wash buffer (50 mM HEPES, pH 7.6, 150 mM NaCl, 5% glycerol, 20 mM imidazole, 1 mM β ME) on a Bio-Rad Biologic FPLC system. Proteins were eluted from the column over two steps, first a linear gradient of 0–100% elution buffer (50 mM HEPES, pH 7.6, 150 mM NaCl, 5% glycerol, 300 mM imidazole, 1 mM β ME) over 60 min, followed by a 100% elution buffer wash for 30 min at 1 mL/min. Fractions containing the purified protein were pooled and loaded onto a HiPrep 16/60 Sephacryl S-200 HR gel filtration column equilibrated with gel filtration buffer (50 mM HEPES, pH 7.6, 150 mM NaCl, 1 mM β ME). Gel filtration was performed by running 1.7 column volumes (CVs) of gel filtration buffer at 0.4 mL/min after protein samples were injected into the column. Fractions containing purified proteins were pooled and concentrated with 10 kDa molecular weight cut-off (MWCO) Amicon centrifugal filters prior to storage at –80 °C with 5% glycerol. Protein concentrations were determined by a TCA-Lowry assay.²³

Antibodies Used in This Study. The primary antibodies used in this study were mouse anti-Elongin B (1:2000, Santa Cruz Biotechnology, catalog # sc-135895), mouse anti-Elongin C (1:2000, Santa Cruz Biotechnology, catalog # sc-166554), mouse anti-6xHis (1:2000, Proteintech, catalog # 66005-1-Ig), mouse anti-GAPDH (1:3000, ProteinTech, catalog # 60004-1-Ig), mouse anti-FLAG antibody conjugated to Dylight 800 (1:10,000, Rockland, catalog # 200-345-383), rabbit anti-rhPCMT1 (1:1000, noncommercial; a kind gift from Dr. Mark Mamula), rabbit anti-Cul5 (1:2000, Bethyl Laboratories, catalog # A302-173A), goat anti-S-Tag (1:100, GeneTex, catalog # GTX19321), and rabbit anti-FLAG (1:200, Cell Signaling Technology, catalog # 14793).

Secondary antibodies used in this study were goat antimouse IgG (H + L) cross-adsorbed Alexa Fluor 488 (1:2000, Thermo Fisher, catalog # A-11001; Figures 8C and S4), goat antirabbit IgG (H + L) Alexa Fluor Plus 647 (1:2000, Thermo Fisher, catalog # A32733; Figure 7A), donkey antimouse IRDye 800CW (1:10,000, LI-COR, catalog #926-32212; Figure 7B), donkey antirabbit IRDye 680RD (1:10,000, LI-COR, catalog # 926-68073; Figure 7B), and antirabbit horseradish peroxidase (HRP) conjugated (1:100,000, Abcam, catalog # ab6721) visualized with Amersham ECL immunoblotting detection reagent (GE Healthcare, catalog # RPN2106; Figure 6).

Expression and Solubility Trials of PCMTD1 and PCMTD1–EloBC.

Fifty milliliter cultures of either PCMTD1 alone or PCMTD1–EloBC strains were inoculated at a starting OD₆₀₀ of 0.05. When cultures reached 0.5 OD₆₀₀, an uninduced aliquot corresponding to 0.4 OD of cells was removed, and the expression of constructs was induced by the addition of 0.5 mM IPTG. Expression continued for 4.5 h at 37 °C. Then, an induced aliquot corresponding to 0.4 OD of cells was removed and cells were pelleted at 5000g at 4 °C. Cell pellets were resuspended in 12.5 mL of lysis buffer (50 mM HEPES, pH 7.6, 300 mM NaCl, 5% glycerol, 1 mM β ME, 1 mM PMSF, and 1 EDTA-free Pierce protease inhibitor tablet per 50 mL) and lysed using a 550 Sonic Dismembrator at a 50% duty cycle with 15 rounds of 30 s on, 30 s off. Debris was pelleted at 13,000 rpm at 4 °C. The resultant supernatant was removed as the soluble fraction, and the pellet was resuspended in 12.5 mL lysis buffer as the insoluble fraction. Ten microliters of the uninduced, induced, soluble, and insoluble samples were analyzed by SDS-PAGE and anti-His immunoblot detection.

PCMTD1 Degradation Trials within Tetracycline-Treated *E. coli*.

Fifty milliliter expression cultures were inoculated from PCMTD1 or PCMTD1–EloBC overnight cultures at a starting OD₆₀₀ = 0.05. When expression cultures reached OD₆₀₀ = 0.4, uninduced aliquots of cells were removed and expression was induced with 0.5 mM IPTG at 37 °C. After 30 min, an aliquot of cells corresponding to 0.4 OD of cells was taken as an induced sample. Then, tetracycline (Sigma-Aldrich, catalog # T7660) was added at a final concentration of 25 μ g/mL. Aliquots corresponding to 0.4 OD of cells were removed at 10 min, 30 min, 1 h, 2 h, and 3 h time intervals after tetracycline addition and analyzed by both Coomassie staining or Ponceau staining and anti-His immunoblot detection.

[³H]AdoMet:Protein Ultraviolet Light Cross-Linking Experiments.

In a final volume of 60 μ L, 3.85 μ M protein was mixed with 0.5 μ M S-adenosyl-L-[methyl-³H] methionine ([³H]AdoMet; PerkinElmer Life Sciences; 75–85 Ci/mmol, 0.55 mCi/mL in 10 mM H₂SO₄/ethanol (9:1, v/v)) in 50 mM

tris-HCl, pH 7.6. Where indicated in the figure legend, 0.5 mM of either nonradioactive S-adenosylhomocysteine or adenosine triphosphate (ATP) was added. Reactions were placed into NUNC 96-well clear-bottom plates and exposed to 254 nm ultraviolet light at 4 °C for 1 h. The reaction was stopped by adding 15 μ L 5 \times SDS-PAGE sample buffer (250 mM tris-HCl, pH 6.8, 10% SDS, 50% glycerol, 5% β MME, and 0.05% bromophenol blue). Samples were heated at 95 °C for 3 min and separated on a 4–20%, 10-well ExpressPlus PAGE gel (Genscript, catalog # M42010) at 140 V for 1 h. Gels were stained with Coomassie (0.1% (w/v) Brilliant Blue R-250, 10% (v/v) glacial acetic acid, and 50% (v/v) methanol) for 1 h and destained with 10% (v/v) acetic acid and 15% (v/v) methanol. For fluorography, gels were subsequently incubated with EN³HANCE (PerkinElmer Life Sciences, catalog number 6NE9701) for 1 h, incubated in water for 30 min, and dried before the gels were exposed to film (Denville Scientific, 8 \times 10-in. Hyblot Cl) for the length of time designated in the figure legends at –80 °C.

Determination of L-Isoaspartate-Methylation Levels by the Methanol Vapor Diffusion Assay. PCMT1 was used as an analytical reagent to quantify L-isoaspartate levels; it was purified as a His-tagged enzyme from the expression plasmid #34852 available from Addgene.com as described by Patananan et al.²⁴ with a specific activity at 37 °C of 5,300 pmol of methyl esters formed on KASA(isoD)LAKY/min/mg of enzyme. The isoaspartate-containing substrates used in this assay were the synthetic peptide KASA(isoD)LAKY and the protein ovalbumin (SIGMA A5503). In a final volume of 100 μ L, 10 pmol of PCMT1 or 15 pmol PCMTD1–EloBC was incubated with 25 pmol KASA(isoD)LAKY or 500 pmol ovalbumin (typically ~6% isomerized). Final concentrations in the reactions included 135 mM bis-tris-HCl, pH 6.4, and 10 μ M S-adenosyl-L-[methyl-³H]methionine ([³H]AdoMet) (prepared by a 1600-fold isotopic dilution of a stock of 72 Ci/mmol [³H]AdoMet (PerkinElmer Life Sciences, NET155H00) with nonisotopically labeled AdoMet (*p*-toluenesulfonate salt; Sigma-Aldrich A2408)). The reaction was stopped by adding 10 μ L of 2 M sodium hydroxide, and 100 μ L of the 110 μ L mixture was transferred to a 9 \times 2.5 cm² piece of folded thick filter paper (Bio-Rad; catalog number 1650962) wedged in the neck of a 20 mL scintillation vial above 5 mL scintillation reagent (Safety Solve, Research Products International, catalog number 121000), tightly capped, and incubated at room temperature. After 2 h, the folded filter papers were removed, the caps were replaced, and the vials were counted thrice for 5 min each in a Beckman LS6500 scintillation counter. Background radioactivity in a reaction containing no substrate was determined by incubating the recombinant human PCMT1 or PCMTD1–EloBC, 135 mM bis-tris-HCl buffer, and 10 μ M [³H]AdoMet, as described above. Samples were analyzed in triplicate.

Animal Husbandry. *Pcmt1*^{–/–} animals were generated through breeding of *Pcmt1*^{+/-} animals and maintained as reported previously.^{12,25} These animals have been interbred for 20 years to obtain a genetically homogeneous population. *Pcmt1*^{–/–} and *Pcmt1*^{+/+} offspring were used in this study. Mice were kept on a 12 h light/dark cycle and allowed ad libitum access to water and NIH-31 7013 pellet chow (18% protein, 6% fat, 5% fiber, Harlan Teklad, Madison, WI).

Preparation of Wild-Type and *Pcmt1* Knockout Mouse Tissue Lysates. Fifty-two day old wild-type and *Pcmt1* knockout mice were euthanized in a CO₂ chamber.

Brain tissue was removed and weighed, and 5 mL/g tissue of ice-cold lysis buffer (250 mM sucrose, 10 mM tris-HCl, pH 7.4, 1 mM ethylenediaminetetraacetic acid (EDTA), 1 mM phenylmethylsulfonyl fluoride (PMSF); one Roche protease inhibitor cocktail tablet) was added per 50 mL buffer. Tissues were homogenized with a Fisher LR400A Lab-Stirrer with a Potter-Elvehjem Teflon and glass homogenizer at approximately 300 rpm and then spun at 20,000g for 20 min at 4 °C. The supernatant was removed as the soluble extract and stored at –20 °C until future use.

SDS-PAGE Fluorography for the Analysis of Methyltransferase Activity. Twenty-five micrograms of wild-type and *Pcmt1* knockout mouse brain cytosolic proteins were incubated in a 30 μ L reaction volume with 6 μ g recombinant human PCMT1 or PCMTD1–EloBC, and 0.3 μ M S-adenosyl-L-[methyl-³H] methionine (PerkinElmer Life Sciences; 75–85 Ci/mmol, 0.55 mCi/mL in 10 mM H₂SO₄/ethanol (9:1, v/v)) in 74 mM bis-tris-HCl, pH 6.4, for 2 h at 37 °C. The reaction was stopped by adding 5 \times SDS-PAGE sample buffer and boiling at 95 °C for 3 min. Samples were then separated on a gel, and Coomassie staining and fluorography were performed as described above.

Cell Culturing Conditions. HeLa Flp-In TRex and hTERT-RPE-1 cells were maintained in Dulbecco's modified Eagle's medium (DMEM)/F12 media (Hyclone, catalog # SH30023.01) supplemented with 10% fetal bovine serum (FBS) by volume (Atlanta Biological, catalog #S10350; note this FBS contains no detectable tetracycline to avoid expression of the doxycycline-inducible proteins until the addition of doxycycline) and penicillin/streptomycin (Gibco, catalog #15140148). Cells were passaged using trypsin (Gibco, catalog # 25300054) and in cell culture plates (Thermo, catalog #150350 and 140685).

To generate cell lines expressing doxycycline-inducible pGLAP2 PCMTD1 and EGFP, 4 μ g of pOG44 (encoding Flippase recombinase) and 1 μ g of pGLAP2 PCMTD1 or EGFP were transfected with 15 μ L of Fugene 6 (Promega, catalog # E2691) into one well of a six-well plate of HeLa Flp-In TRex cells at 66% confluency. Forty-eight hours after transfection, the cells were expanded into a 10 cm plate and allowed to grow for another 48 h. The cells were selected with 400 μ g/mL of hygromycin B (Gibco, catalog # 10687010) for 2 weeks, whereupon untransfected (control) HeLa Flp-In TRex cells died and hygromycin-resistant colonies were visible in both pGLAP2 PCMTD1 and pGLAP2 EGFP plates. The colonies were allowed to grow in media without hygromycin for 2 weeks before the colonies were pooled together and used for experiments.

Ni-NTA and S-Tag Pulldowns for the Analysis of PCMTD1–Cul5 Interactions *In Vitro* and in Cells. For Ni-NTA pulldowns, 1.12 nmol of N-terminal His-tagged PCMTD1–EloBC or PCMTD1^{1–231} was immobilized by gentle rocking onto 100 μ L HisPur Ni-NTA resin (Thermo Fisher, catalog # 88221) pre-equilibrated with wash buffer (50 mM HEPES, pH 7.6, 150 mM NaCl, 5% glycerol, 1 mM β MME, 20 mM imidazole) for 1 h at RT. hTERT-RPE-1 (retinal pigment epithelial cells) cell lysate samples were then freshly prepared by incubating 110 μ L cell lysis buffer (50 mM HEPES, pH 7.6, 150 mM NaCl, 1 mM PMSF, 1% NP40, 1 mM β MME) with 3 \times 10⁶ hTERT-RPE-1 cells (lysate C_F ~ 0.4 mg/mL) on ice for 12 min with gentle mixing. Lysates were then cleared by a 13,300g spin at 4 °C for 10 min. Following immobilization of purified proteins to the Ni-NTA resin, 110

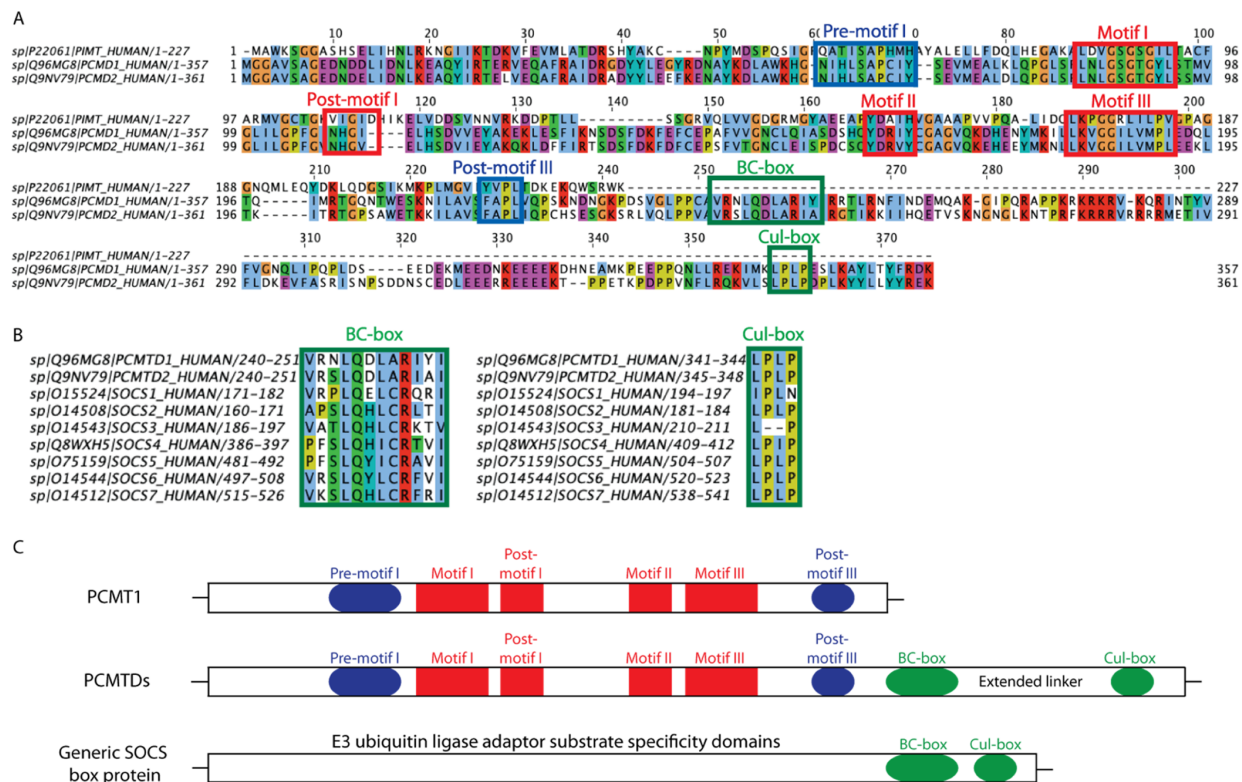


Figure 1. Sequence alignment of human PCMT1 (PIMT), the PCMTD proteins, and SOCS box proteins. (A) Sequence alignment of PCMT1 with PCMTD1 and PCMTD2. For conserved residues, the color scheme is as follows: hydrophobic (blue), positive charge (red), negative charge (magenta), polar (green), cysteine (pink), glycine (orange), proline (yellow), and aromatic (cyan). Sequences outlined in blue correspond to PCMT1 isoaspartyl-binding motifs, while sequences outlined in red represent PCMT1 AdoMet binding motifs. Residues boxed in green in the PCMTD proteins comprise the BC-box and Cul5 box binding motifs of the SOCS box domain. (B) Sequence alignment of the C-terminal region of PCMTD1 and PCMTD2 (residues 225–357) with the SOCS box proteins. Residues boxed in green comprise the BC-box and Cul5 box binding motifs of the SOCS box domain. (C) Domain comparison of PCMT1, the PCMTDs, and SOCS box proteins. Blue boxes correspond to PCMT1 isoaspartyl-binding motifs, red boxes correspond to PCMT1 AdoMet binding motifs, and green boxes represent the BC-box and Cul5 box binding motifs of the SOCS box domain.

μ L of cell lysate was directly added to the Ni-NTA resin and rocked for 2 h at RT. The resin was then washed three times. After the final wash, immobilized proteins and potential binding partners were eluted with 160 μ L elution buffer (50 mM HEPES, pH 7.6, 150 mM NaCl, 5% glycerol, 1 mM β ME, 300 mM imidazole). Samples were then analyzed by Coomassie staining and immunoblot detection.

For S-Tag pull-downs, two wells of a six-well plate each of HeLa pGLAP2 PCMTD1 and pGLAP2 EGFP were plated at a 66% confluency. For each cell line, one well was left without doxycycline as a control, and to the other well, 0.1 μ g/mL of doxycycline was added for 18 h. The cells were lysed in 120 μ L LAP200 buffer supplemented with dithiothreitol (DTT), protease inhibitors, and 1% NP40. Five microliters of lysate was added to 2 μ L of 6 \times Laemmli buffer and boiled for 5 min at 95 $^{\circ}$ C. From the remaining doxycycline-induced lysates, 110 μ L was added to 50 μ L of S-protein agarose beads (Millipore, catalog # 69704) in 250 μ L of LAP200 without NP40 (for a final concentration of about 0.3% NP40) and allowed to bind, rotating end over end, for 2 h at 4 $^{\circ}$ C. The beads were pelleted by centrifugation at 500g for 2 min at 4 $^{\circ}$ C and washed with 250 μ L of LAP200 with 0.33% NP40 four times. After the final wash, the beads were pelleted, the supernatant was aspirated, and 20 μ L of 6 \times Laemmli buffer was added. The beads were

boiled for 5 min at 95 $^{\circ}$ C. The resulting proteins were subjected to SDS-PAGE and immunoblot detection.

CRL5–PCMTD1 Complex Constitution and Analytical Gel Filtration Chromatography. CRL5–PCMTD1 was made by incubating Cul5–Rbx2 and PCMTD1–EloBC at a molar ratio of 1:1:1 for 2 h at room temperature with gentle rocking. CRL5–PCMTD1, Cul5–Rbx2, and PCMTD1–EloBC were then concentrated to 0.2 mg/mL prior to analytical gel filtration chromatography. Four hundred microliters of concentrated samples were then injected and ran on a Superdex 200 Increase 10/300 GL column with an AKTApriime plus FPLC system for 2 CVs with gel filtration buffer (50 mM HEPES, pH 7.6, 150 mM NaCl, 5% glycerol, 1 mM β ME at 0.3 mL/min).

Native-PAGE. Protein samples for native-PAGE were prepared by mixing four parts of protein sample with one part of 5 \times native sample buffer (124 mM tris base, pH 6.8, 3.8 mM bromophenol blue, 50% glycerol, 1.43 M β ME) without heating. Five micrograms of total protein was loaded onto a 10-well 4–20% gel (Genscript, catalog # M42010). Gels were electrophoresed with a native running buffer (50 mM tris, pH 7.4, 50 mM 3-(*N*-morpholino)propanesulfonic acid (MOPS), 1 mM EDTA) at 30 V until the dye front migrated to the

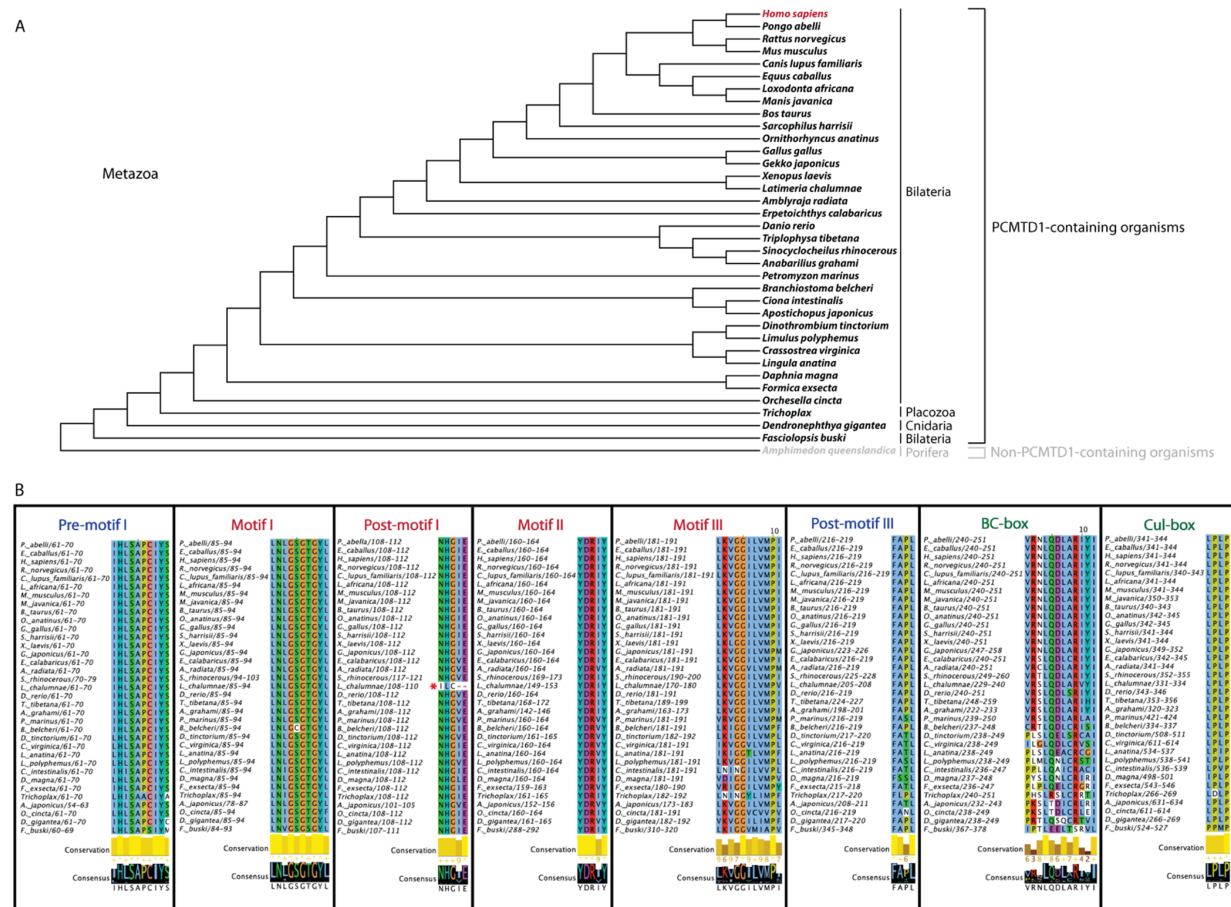


Figure 2. PCMTD1 is present within select metazoan phyla and is well conserved in most chordate organisms. (A) A protein BLAST search was performed against PCMTD1 isoform 1. At least one species from each phylum that was identified were selected, and a multiple sequence alignment was performed. Organisms are designated as belonging to the superphyla bilateria, cnidaria, or placozoa. A PCMT1-like protein lacking any similar PCMTD1 C-terminal domain was identified in porifera and used to root the tree; no significant matches were identified in ctenophora. The phylogenetic tree of the full-length PCMTD1 sequences was generated utilizing the maximum likelihood method in MEGAX, as described in the Experimental Procedures and rooted in the outgroup species *Amphimedon queenslandica* PCMT1-like protein. (B) T-Coffee multiple sequence alignment of PCMTD1 motifs from the selected organisms in panel (A). AdoMet binding motifs are labeled in red, L-isospartyl recognition motifs are labeled in blue, and SOCS box motifs are labeled in green. For conserved residues, the color scheme is as follows: hydrophobic (blue), positive charge (red), negative charge (magenta), polar (green), cysteine (pink), glycine (orange), proline (yellow), and aromatic (cyan).

bottom of the gel. Gels were then stained and destained with Coomassie as described above.

RESULTS

PCMTD Proteins Contain Both L-Isoaspartyl Methyltransferase and Cullin-RING Ligase Motifs. Figure 1A displays an alignment of the primary sequences of human PCMT1 (227 residues), PCMTD1 (357 residues), and PCMTD2 (361 residues). PCMTD1 and PCMTD2 share approximately 26% similarity with PCMT1. Similar regions include both motifs common for seven β-strand methyltransferases and motifs specific for L-isospartyl binding.²⁶ Notably, PCMTD1 and PCMTD2 contain several conserved residues which directly interact with isoaspartyl substrates and AdoMet through hydrogen-bonding and hydrophobic interactions (Figure 1A).²⁷ However, PCMTD1 and PCMTD2 have ~130 additional residues comprising a novel C-terminal domain. Encompassed within the additional ~130 amino acids of the PCMTD proteins are two motifs that comprise the

SOCS box recruitment domain: the BC-box and the Cul-box that are found in E3 ubiquitin ligases. Both of these motifs align well with other human SOCS box proteins, with the PCMTD1 BC-box and Cul-box motifs having an average of 54 and 73% sequence identities, respectively, compared across the seven human SOCS proteins (Figures 1B and S1). The BC-box is a 12-residue motif that recruits proteins Elongin B and Elongin C, which are Cullin-RING E3 ubiquitin ligase adaptor proteins. Elongins B and C form a heterodimer, which mediates interactions between SOCS box-containing proteins with Cul5 to form a partial Cullin-RING E3 ubiquitin ligase complex.²⁸ A leucine at the +4 position within the BC-box has been shown to be critical for this interaction^{29,30} and is conserved within the sequences of both PCMTD1 and PCMTD2 (Figures 1B and S1). In contrast to other SOCS box-containing proteins, which contain an 11-residue spacer separating the Cul- and BC-boxes, the Cul-box in PCMTD1 and PCMTD2 is separated from the BC-box by ~90 residues,

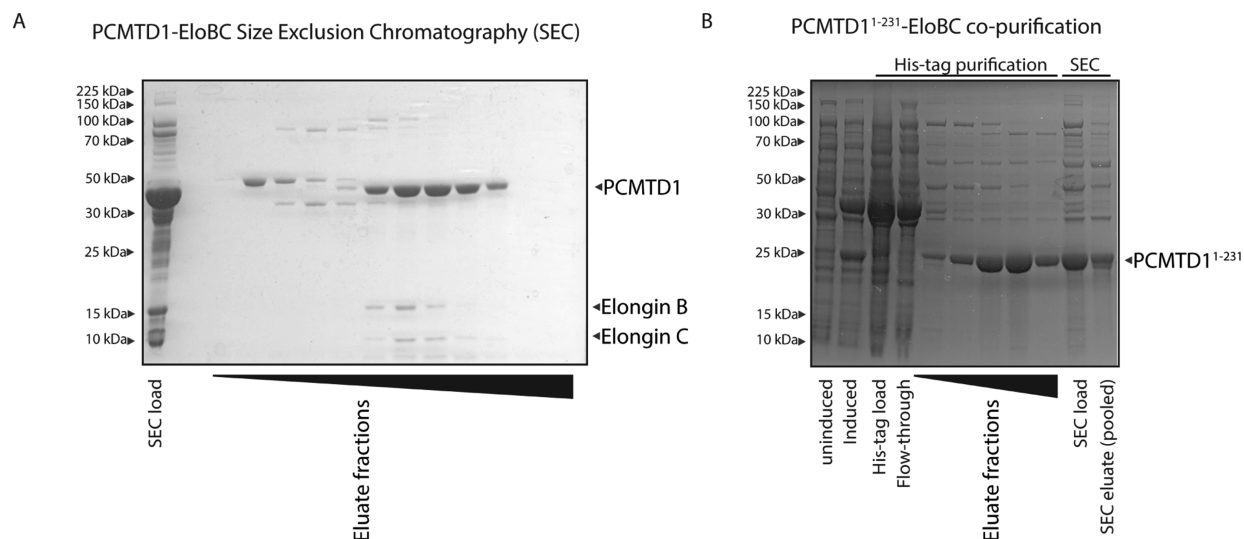


Figure 3. C-terminus of PCMTD1 facilitates interactions between PCMTD1 and Elongins B and C. (A) SDS-PAGE results of sequential fractions collected during size exclusion chromatography of His-tag purified preparations of PCMTD1–EloBC reveal that PCMTD1 and Elongins B and C coeluted as a complex. (B) His-tag purification and size exclusion chromatography result in the purification of PCMTD1^{1–231} alone when PCMTD1^{1–231} is coexpressed with Elongins B and C. This suggests that PCMTD1^{1–231} does not interact with Elongins B and C.

which generates a novel extended SOCS box motif (Figure 1C).

PCMTD1 Is Present within Certain Metazoan Phyla and Is Highly Conserved in Chordates. Using BLAST and phylogenetic analyses, a tree was generated displaying PCMTD1 protein sequence similarities from select organisms representative of all phyla in which PCMTD1 was identified (Figure 2A).³¹ Unlike the PCMT1 methyltransferase, which is present within bacteria, archaea, and eukaryota, PCMTD1 was only found within select phyla of the metazoan kingdom.²⁴ Specifically, this previously uncharacterized protein was found within the superphyla bilateria, cnidaria, and placozoa but not within ctenophora, porifera, nor choanoflagellata. Interestingly, SOCS box-containing proteins have been identified in bilateria, cnidaria, placozoa, ctenophora, and porifera, in addition to a putative SOCS box-containing protein found in the choanoflagellate *Salpingoeca rosetta*.^{32,33} These observations may suggest that the PCMTD proteins originated from a gene duplication event within the last common ancestor of the bilateria, cnidaria, and placozoa superphyla. Phylogenetic analysis indicates that the human PCMTD1 sequence is on average 76% identical to sequences across the chordate phylum (Figure 2A). PCMTD1 sequence alignment across representative organisms is shown in Figure 2B. Across all phyla shown, the AdoMet binding motifs and the L-isoaspartyl recognition motifs are on average 88 and 89% identical, respectively (Figure 2B). While the Cul-box of the SOCS box motif is 92% identical, there is more variation within the BC-box at 62% identity averaged across the species shown here. At this point, it is unclear what the roles of the variant BC-box are in lower organisms. However, the +4 leucine is perfectly conserved within the BC-box, suggesting strong positive selective pressure. This residue is also conserved across all human SOCS box-containing proteins (Figure S1).

As mentioned above, the human PCMTD1 and PCMTD2 sequences represent a unique extension of the canonical SOCS box motifs due to the insertion of +90 residues between the BC-box and the Cul-box, compared to the canonical +11

residues within previously characterized SOCS box-containing proteins (Figures 1B and S1B). Interestingly, the tunicate *Ciona intestinalis*, the arthropods *Daphnia magna*, *Formica exsecta*, *Limulus polyphemus*, *Dinorthis tinctorium*, and *Orchesella cincta*, the mollusk *Crassostrea virginica*, and the echinoderm *Apostichopus japonicus* each has over 200 residues between the BC-box and the Cul-box of their PCMTD1 sequences, with the longest distance being 386 residues within *A. japonicus*. In stark contrast, the cnidarian *Dendronephthya gigantea* and the placozoan *Trichoplax*, which are approximately as distantly related to humans as the previously listed organisms, have 15 and 12 residues extending between their BC- and Cul-boxes. Within these elongated interim sequences, there are several stretches with conserved residues including a positive patch corresponding to residues 275-KRKRKR-280 in the human PCMTD1 sequence (Figure S2C), as well as a highly negative patch corresponding to residues 303-EEDKMEEDNKEEEEKD-319 in the human PCMTD1 sequence (Figure S2G–L). The positive and negative patches within the human PCMTD1 sequence are on average 96 and 61% similar to the other chordate sequences, respectively.

A protein BLAST query of the linker region of the nonredundant protein database using human PCMTD1 residues Arg252–Lys340 did not reveal significant sequence similarities with any non-PCMTD proteins. The C-terminal domains of both human PCMTD1 and PCMTD2 are predicted to exist as independent isoforms lacking the methyltransferase domain (PCMTD1 isoform 2 and PCMTD2 isoform 3, respectively), resulting from alternative splicing (Figure S3).^{34–37} Given the presence of the BC-box, the Cul-box, and the large region of residues with unknown purposes, it is possible that these are active isoforms with distinct functions from the full-length PCMTD proteins.

Recombinant Human PCMTD1 Expression Is Stabilized by Coexpression with Elongins B and C. The BC-box found within the SOCS box motif is conserved for Elongins B and C binding. To investigate the function of the BC-box identified within the PCMTD1 sequence, His-tagged

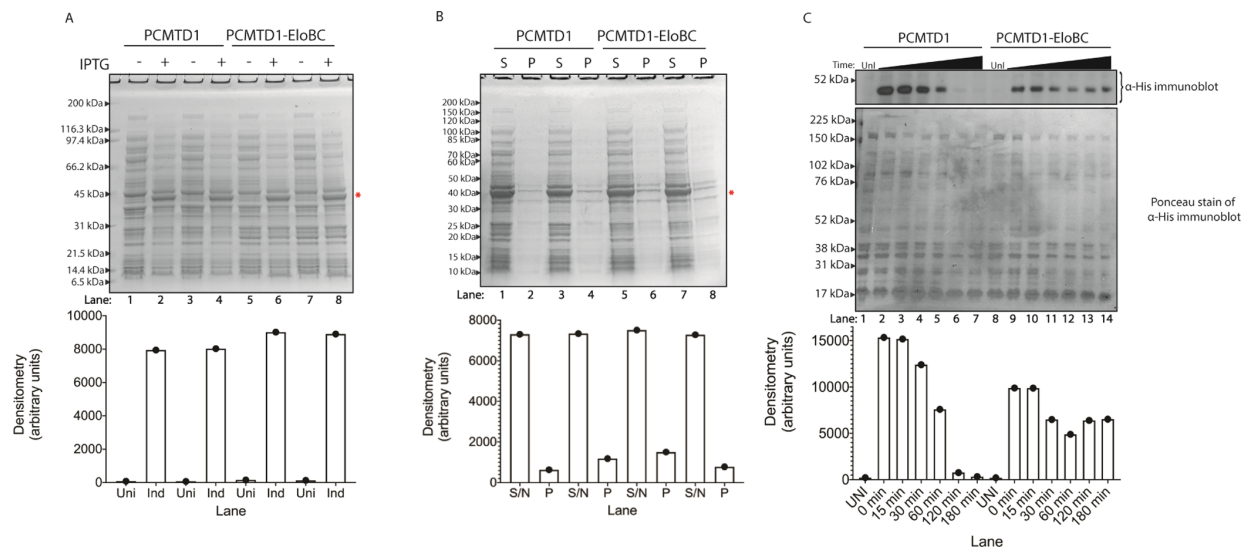


Figure 4. Elongins B and C help stabilize recombinant PCMTD1. (A) Coomassie-stained SDS-PAGE gel of PCMTD1 IPTG-induced expression with (lanes 6 and 8, replicates) and without Elongins B and C from whole cell lysates (lanes 2 and 4, replicates). The lower panel represents densitometric quantification of the PCMTD1 band (indicated by a red asterisk). (B) Coomassie-stained SDS-PAGE gel of the supernatant (S) and pellet (P) of lysed *E. coli* expressing either PCMTD1 alone (lanes 1–4) or PCMTD1–EloBC (lanes 5–8). The lower panel represents densitometric quantification of the PCMTD1 band indicated by a red asterisk. (C) *E. coli* cells expressing PCMTD1 alone (lanes 1–7) or PCMTD1 with Elongins B and C (lanes 8–14) were treated with 25 $\mu\text{g}/\text{mL}$ tetracycline, as described in the [Experimental Procedures](#) section. Lanes 1 and 8 represent whole cell lysates from uninduced cultures. Succeeding lanes represent whole cell lysates from induced cultures treated with tetracycline at increasing time points. The lower panel represents densitometric quantification of the PCMTD1 band detected by an anti-His immunoblot.

PCMTD1 was recombinantly coexpressed with untagged Elongins B and C proteins in *E. coli* (Figure 3A). PCMTD1 and Elongins B and C were purified within the same fractions in immobilized metal affinity chromatography and size exclusion chromatography (Figures 3A and S4A). Thus, the association and complex formation between PCMTD1 and Elongins B and C, now termed PCMTD1–EloBC, were demonstrated (Figure 3A). Cotransformation and subsequent coexpression of a C-terminally truncated construct of His-tagged PCMTD1, PCMTD1^{1–231}, and Elongins B and C in *E. coli* resulted in the purification of PCMTD1^{1–231} alone after size exclusion chromatography (Figures 3B and S4B). These results suggest that the BC-box found within the C-terminus of PCMTD1 facilitates the interactions between PCMTD1 and Elongins B and C.

For SOCS box-containing proteins, several regions responsible for the E3 ubiquitin ligase complex association have been suggested to be intrinsically disordered in the absence of Elongins B and C.^{38–40} To investigate the nature of the effects Elongins B and C may have on PCMTD1 expression, recombinant expression trials for constructs of PCMTD1 alone and PCMTD1 coexpressed with Elongins B and C were compared in duplicate *E. coli* cultures. Uninduced and induced whole cell lysates were analyzed by SDS-PAGE (Figure 4A). Densitometry of the band corresponding to induced PCMTD1 suggested that there were modest increases of $\sim 11\%$ in the expression or stability of PCMTD1 with the coexpression of the Elongins (Figure 4A, lower panel). The lysates from induced cultures were then separated into soluble supernatant (S) and insoluble pellet (P) fractions. These samples were analyzed by SDS-PAGE, and densitometry performed on the band corresponding to PCMTD1 revealed no detectable increases in the solubility of PCMTD1 with the Elongins. To

explore the stability of the PCMTD1 protein, *E. coli* cultures were grown to mid-log phase and the PCMTD1 constructs were induced with IPTG. After 30 min of expression, the protein synthesis inhibitor tetracycline was added to cells and aliquots of the culture were taken at increasing time points. Lysates were separated by SDS-PAGE, and levels of PCMTD1 were evaluated by both Coomassie stain and immunoblot against the N-terminal His-tag (Figure 4C). While the PCMTD1-alone culture has higher initial signal at 30 min of expression, the protein levels decrease steeply after 1 h of treatment with tetracycline and are completely depleted after 2 h (Figure 4C, lanes 2–7). Strikingly, while the PCMTD1–EloBC samples display lower levels of initial signal, His-PCMTD1 could be detected by immunoblot throughout the course of the tetracycline treatment (Figure 4C, lanes 9–14). This result was replicated, indicating that the Elongins help stabilize recombinant PCMTD1 protein levels (Figure S5). Thus, all subsequent *in vitro* experiments were performed with the recombinantly coexpressed complex of PCMTD1 and Elongins B and C (PCMTD1–EloBC; Figure 4).

PCMTD1–EloBC Specifically Binds to the Methyltransferase Cofactor AdoMet. To assess possible binding between AdoMet and PCMTD1, PCMTD1–EloBC or PCMTD1^{1–231} purified proteins were incubated with S-adenosyl-[methyl-³H]-L-methionine ([³H]AdoMet) and exposed to a UV light source with or without the addition of S-adenosylhomocysteine (AdoHcy) or adenosine 5′triphosphate (ATP). Cross-linking results were then monitored with SDS-PAGE and fluorography. Signals observed on the film correspond to the PCMTD1 band within the gel, indicating that PCMTD1–EloBC is able to cross-link to [³H]AdoMet (Figure 5). Addition of the methyltransferase site-specific inhibitor, AdoHcy, inhibited cross-linking between [³H]-

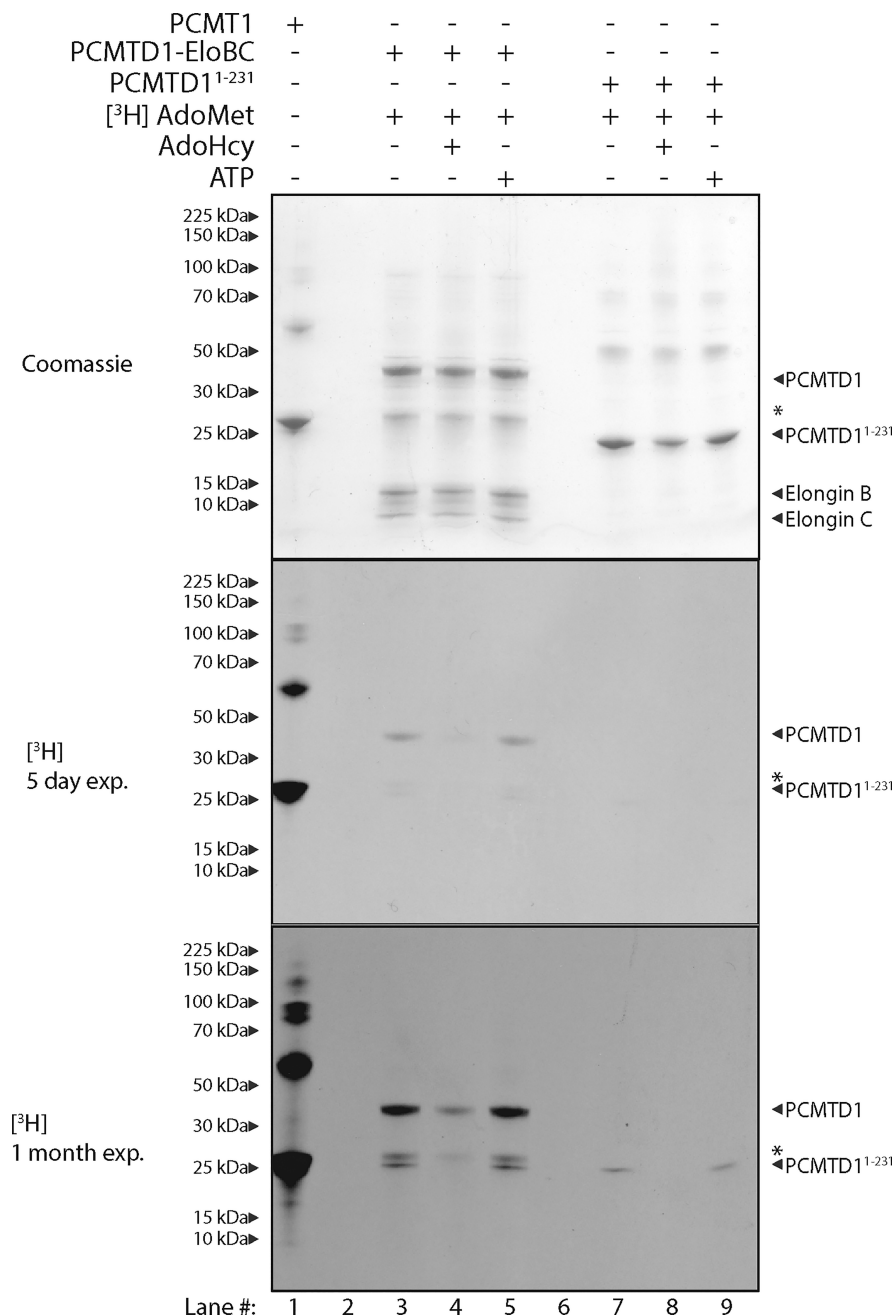


Figure 5. PCMTD1 site-specifically binds [³H]AdoMet. The Coomassie-stained SDS-PAGE gel (upper panel) and fluorography (lower two panels) show [³H]AdoMet cross-linked to the PCMT1 positive control (lane 1), PCMTD1–EloBC (lanes 3 and 5), and PCMTD1^{1–231} (lanes 7 and 9) at pH 7.6. A known inhibitor of site-specific [³H]AdoMet binding to PCMT1 (AdoHcy) was able to abrogate [³H]AdoMet binding for both PCMTD1–EloBC (lane 4) and PCMTD1^{1–231} (lane 8). ATP was not able to inhibit binding between PCMTD1–EloBC or PCMTD1^{1–231} to [³H]AdoMet (lanes 5 and 9). The film was exposed for 5 days (middle panel) and 30 days (lower panel) for the same experiments. Asterisks indicate potential PCMTD1 degradation products.

AdoMet and PCMTD1–EloBC. However, ATP did not inhibit binding. Together, these results suggest that PCMTD1–EloBC is able to site-specifically cross-link to [³H]AdoMet. PCMT1 exhibits similar binding behavior, whereas bovine serum albumin, a negative control, exhibits no binding activity to [³H]AdoMet in cross-linking reactions (data not shown).

Performing these experiments with the truncated PCMTD1^{1–231} variant shows that AdoMet binding is localized in the PCMT1-homologous N-terminus of PCMTD1. PCMTD1^{1–231} similarly cross-links [³H]AdoMet in a site-specific manner (Figure 5). The signal for binding was lower in comparison to PCMTD1–EloBC. This may be caused by allosteric effects induced by the interactions between

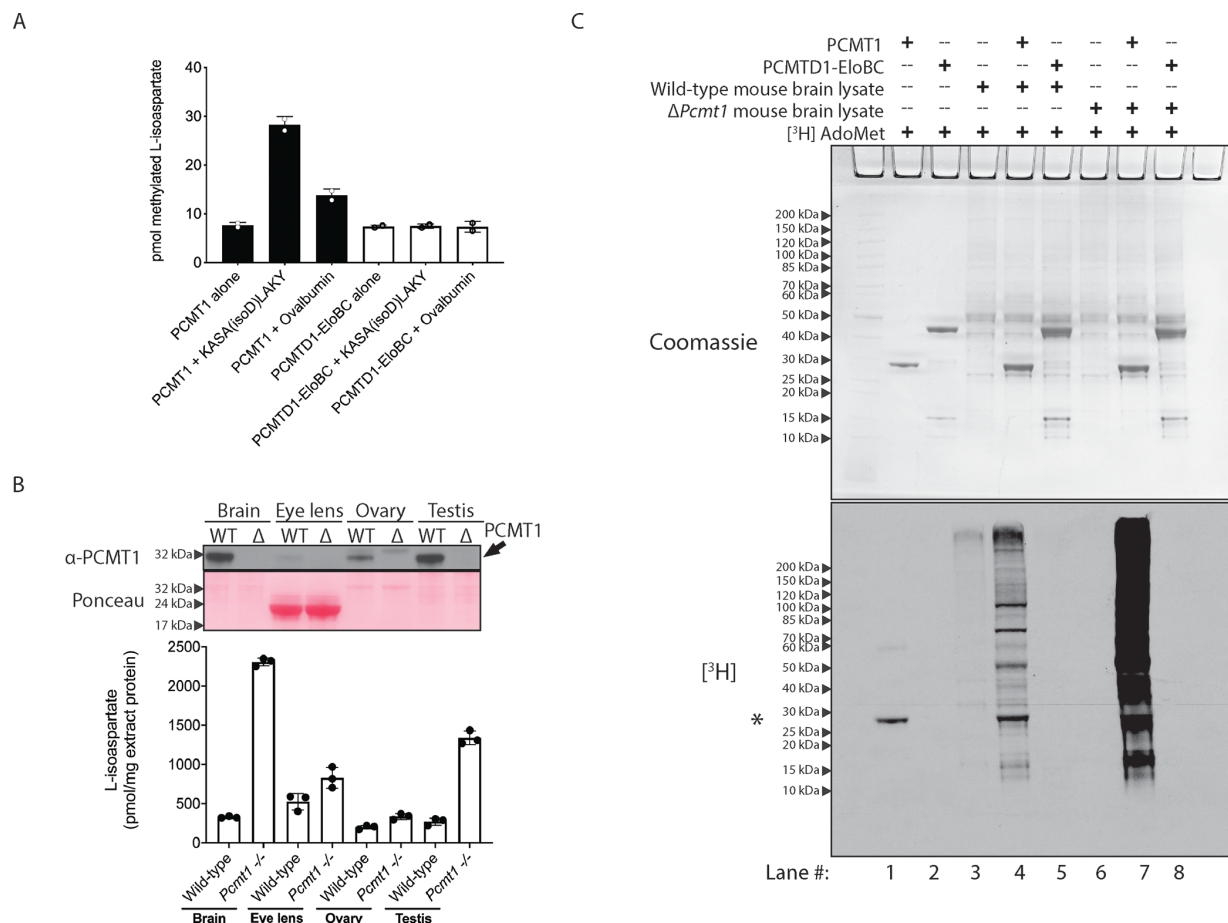


Figure 6. PCMTD1–EloBC does not display methyltransferase activity. (A) L-Isoaspartate-specific methylation of 30 pmol of the KASA(isoD)LAKY peptide and 500 pmol of ovalbumin were detected by a methanol vapor diffusion assay, as described in the [Experimental Procedures](#). The assay was performed in duplicate; error bars represent range. (B) Mouse tissue extracts from wild-type (WT) or $\Delta Pcm1$ mice were tested for the presence of PCMT1 with an anti-*rh*PCMT1 antibody (upper panel). The extracts were then tested for L-isoaspartate content using the vapor diffusion assay, as described in the [Experimental Procedures](#). Assays were performed in triplicate; error bars represent standard deviation. (C) Total methylation was investigated by incubation of proteins with S-adenosyl-L-[methyl- 3 H] methionine ([3 H]AdoMet) and either wild-type mouse brain lysate or *Pcm1* knockout mouse brain lysate, as described in the [Experimental Procedures](#). All [3 H]-labeled proteins were separated by sodium dodecyl sulfate-polyacrylamide gel electrophoresis (SDS-PAGE). Proteins were visualized by Coomassie staining (upper panel), and [3 H]-methylated proteins were detected by fluorography (lower panel) by exposure to film for 6 days. Asterisk represents PCMT1 automeylation.

PCMTD1 and the adaptor proteins, Elongins B and C. These effects may enhance binding between AdoMet and PCMTD1–EloBC when compared to AdoMet binding of the truncated variant of PCMTD1.

PCMTD1–EloBC Complex Does Not Display Methyltransferase Activity. The sequence conservation of the AdoMet- and L-isoaspartyl-binding sites between PCMT1 and PCMTD1 suggests that this protein may retain similar L-isoaspartyl-methylation activity. Using L-isoaspartate-containing peptide and protein substrates of the canonical repair enzyme PCMT1, we tested for L-isoaspartyl methylation by PCMTD1–EloBC *via* a methanol vapor diffusion assay, which takes advantage of the greater base lability of isoaspartyl methyl esters compared to other sites of methylation (Figure 6A). The canonical L-isoaspartyl repair methyltransferase PCMT1 is able to methylate the synthetic L-isoaspartyl-containing peptide KASA(isoD)LAKY at a near 1:1 stoichiometric ratio. In addition, PCMT1 was able to methylate ovalbumin, a known

PCMT1 substrate, at an \sim 3% stoichiometric ratio, which is consistent with previous studies (Figure 6A).⁴¹ Incubation of substrates with the PCMTD1–EloBC, however, did not show any methylation of L-isoaspartate above the enzyme-alone background (Figure 6A). Furthermore, methylation activity is not observed with the truncated variant of PCMTD1 in similar assays (data not shown).

It is possible that the KASA(isoD)LAKY peptide and the ovalbumin protein are not preferred L-isoaspartate substrates for PCMTD1 or that it is a protein methyltransferase that does not methylate L-isoaspartate residues. To test these hypotheses, we incubated PCMT1 and PCMTD1–EloBC with mouse tissue lysates and [3 H]AdoMet. Using [3 H]AdoMet at an undiluted specific activity of \sim 80 Ci/mmol, it would be possible to detect as little as 1 fmol of methylated product (176 dpm). Tissue extracts from both *Pcm1* $^{-/-}$ mice and WT mice were prepared from brain, eye lens, ovaries, and testes. PCMT1 was then used to quantify L-isoaspartate levels within

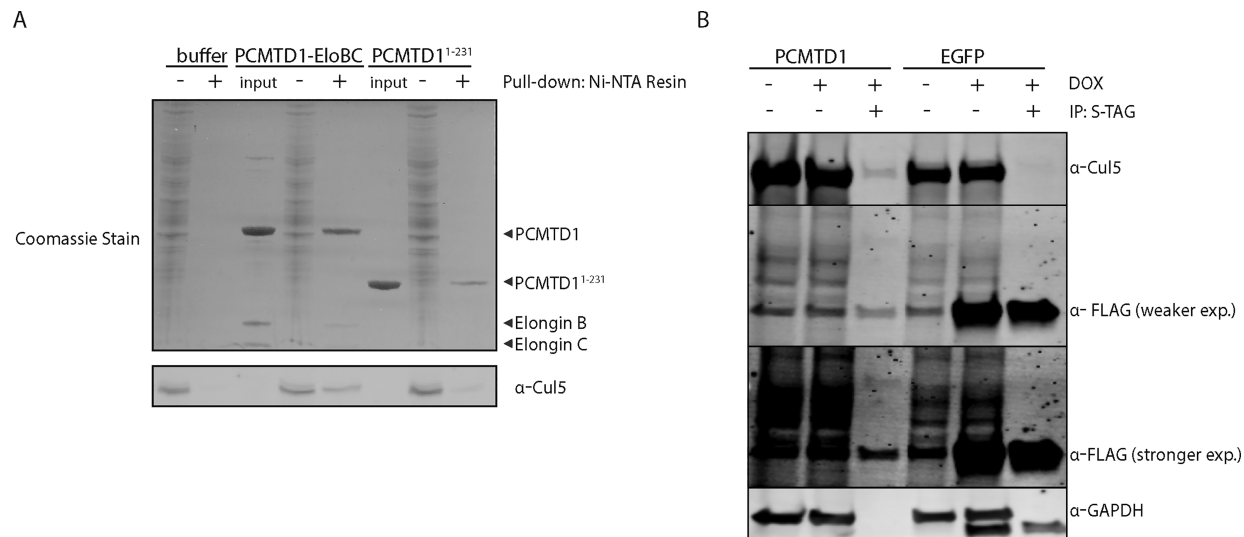


Figure 7. PCMTD1 associates with Cul5 *in vitro* and in cells. (A) PCMTD1's interaction with Cul5 was verified *in vitro* using pull-down assays where recombinant purified proteins were immobilized to Ni-NTA resin as bait. Input lanes represent purified protein stocks used as bait protein that was immobilized onto Ni-NTA resin for pull-down assays. Fresh RPE-1 lysates used as prey are indicated by adjacent – lanes. Proteins eluted from Ni-NTA resin are indicated by the + lanes. The bait proteins were able to coimmunoprecipitate Cul5 as shown by immunoblotting. (B) PCMTD1 was also able to associate with Cul5 in cells. FLAG-S-Tag-PCMTD1 or EGFP expression was induced with 0.1 μg/mL doxycycline in HeLa cells, and the resulting lysates were subjected to immunoprecipitation against the S-Tag and blotted for the indicated proteins. FLAG-S-Tag-PCMTD1, but not FLAG-S-Tag-EGFP, was able to coimmunoprecipitate Cul5. The blot was not stripped between the different antibodies, so the EGFP band is still present in the GAPDH image.

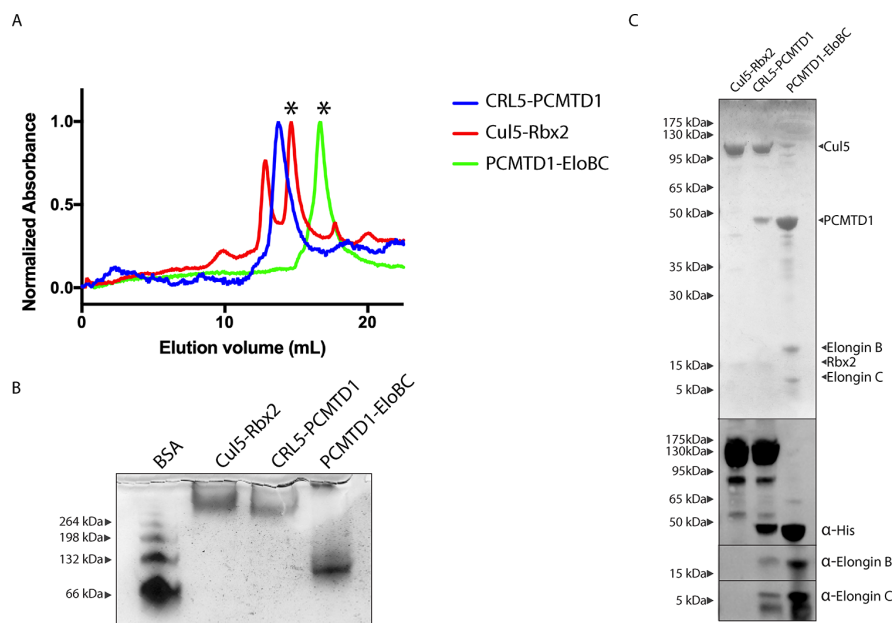


Figure 8. PCMTD1-EloBC interacts with Cul5-Rbx2 to form a PCMTD1-EloBC-Cul5-Rbx2 (CRL5-PCMTD1) complex. (A) Analytical gel filtration suggests that the Cul5-Rbx2 and PCMTD1-EloBC subcomplexes interact to form a larger complex. The CRL5-PCMTD1 complex was formed by incubating purified preparations of Cul5-Rbx2 to PCMTD1-EloBC at a 1.1:1 molar ratio for 2 h at room temperature (RT). Asterisks (*) indicate fractions used for creating this complex. The elution profile CRL5-PCMTD1 (green), PCMTD1-EloBC (blue), and Cul5-Rbx2 (red) were then determined with analytical gel filtration in separate runs. The shift to an earlier elution volume for CRL5-PCMTD1 compared to that for Cul5-Rbx2 and PCMTD1-EloBC suggests that some interaction between these subcomplexes occurs. (B) Shifts in gel mobility and banding pattern in native-PAGE further suggest that a complex is formed between PCMTD1-EloBC and Cul5-Rbx2. (C) SDS-PAGE followed by Coomassie staining and immunoblotting of the singular blue peak or peaks indicated by an asterisk (*) after gel filtration reveal that the blue peak collected during gel filtration contains all protein components for CRL5-PCMTD1.

proteins in each extract sample (Figure 6B). Because *Pcmt1*^{-/-} mice brain extracts contained the highest level of *L*-isoaspartate protein damage overall, this tissue extract was used for subsequent assays (Figure 6B). In the lanes containing *Pcmt1*^{-/-} mouse brain extract and repair enzyme PCMT1, a significant signal as a result of methylation was observed. As expected, methylation signal was more intense in reactions with PCMT1 and brain extract from *Pcmt1*^{-/-} mice (lanes 4 and 7, Figure 6C). Due to endogenous PCMT1 homologues present in WT mice, the background methylation signal was seen in WT mouse brain lysate but was absent in *Pcmt1*^{-/-} mice. In lanes 5 and 8 in which PCMTD1–EloBC was incubated with WT and *Pcmt1*^{-/-} lysates, no significant signal is observed above the lysate-alone lanes 3 and 6. Thus, while the PCMTD1–EloBC complex is able to bind AdoMet, it does not exhibit any detectable protein methyltransferase activity in these *in vitro* assays.

PCMTD1 Associates with Known Components of the Cullin-RING E3 Ubiquitin Ligase. The PCMTD1 C-terminus contains the SOCS box domain, which facilitates the formation of a Cullin-RING E3 ubiquitin ligase complex within SOCS box-containing proteins (Figure 1). Within this domain, the BC-box is responsible for recruiting the heterodimeric adaptor proteins Elongin B and C.²⁸ As shown above, *E. coli* cotransformed with plasmids expressing full-length PCMTD1 and Elongins B and C allowed for the purification of complexed PCMTD1–EloBC. Within the SOCS box, the Cul-box motif further mediates the complex formation between SOCS box-containing proteins and Cul5. To investigate interactions with Cullin-RING ligase component proteins, His-tagged PCMTD1–EloBC was immobilized onto the Ni-NTA resin. We found that recombinant Ni-NTA-immobilized PCMTD1–EloBC was able to pulldown and coelute endogenous Cul5 from RPE-1 cell lysates, as demonstrated with an anti-Cul5 immunoblot (Figure 7A). Using the truncated PCMTD1^{1–231} construct, only a small amount of Cul5 coimmunoprecipitation was seen. These results suggest that the recombinant PCMTD1–EloBC interacts with Cul5 and these interactions may be facilitated by the C-terminus of PCMTD1. To investigate whether Cul5 could interact with PCMTD1 in human cells, HeLa cell lines expressing doxycycline-inducible FLAG- and S-tagged PCMTD1 or EGFP were generated. Tagged PCMTD1 and EGFP were precipitated with S-protein agarose beads, and the subsequent immunoblots were probed for endogenous Cul5. Cul5 coprecipitated with PCMTD1 but not with EGFP (Figure 7B). This suggests that complex formation may occur between PCMTD1 and Cul5 within human cell lysates.

To test whether PCMTD1 is truly capable of forming a complete Cullin-RING E3 ligase complex with Cul5 and Rbx2 *in vitro*, recombinantly purified preparations of Cul5–Rbx2 and PCMTD1–EloBC were incubated together to promote oligomerization into PCMTD1–EloBC–Cul5–Rbx2 (CRL5–PCMTD1). This sample was then chromatographed on an analytical gel filtration column. The CRL5–PCMTD1 complex elutes earlier than Cul5–Rbx2 and PCMTD1–EloBC when chromatographed under identical conditions (Figure 8A). These results suggest that Cul5–Rbx2 and PCMTD1–EloBC do indeed oligomerize to form a larger complex *in vitro*. Native-PAGE analysis of these samples suggests that protein migration behavior of CRL5–PCMTD1 resembles Cul5–Rbx2 more than PCMTD1–EloBC (Figure 8B). This may be caused by particle shape differences in

comparison with CRL5–PCMTD1 to PCMTD1–EloBC—oligomerization into the larger complex may cause CRL5–PCMTD1 to adopt a nonglobular shape that may be important for its proposed enzymatic functions. SDS-PAGE followed by Coomassie staining and immunoblotting verifies that the CRL5–PCMTD1 peak collected during analytical gel filtration does indeed contain the proposed protein components needed for constituting the CRL5–PCMTD1 complex (Figure 8C). Together, these results suggest that PCMTD1 is indeed capable of forming an E3 ubiquitin ligase complex through direct interactions with these CRL proteins, which is reminiscent of other substrate adaptor proteins implicated in the Cullin-Ring E3 ligase family.

DISCUSSION

Disruption of protein homeostasis by protein misfolding or aggregation can be the result of numerous factors including cellular stress, inherited mutations, or protein aging. Aging can contribute to errors within protein homeostasis through the damage and aggregation of long-lived proteins and through the disruption of the protein homeostasis network.⁴² A thorough understanding of the proteins involved in this network and their substrates helps inform the therapeutic design for related diseases.⁴³ The function of the PCMTD1 and PCMTD2 proteins was previously proposed to be a link between the methylation and ubiquitylation of the protein age-related modification, *L*-isoaspartate, based on their interactions with Elongins and Cullins.⁴⁴ However, we have not detected any methyltransferase activity for these proteins. PCMTD1 and PCMTD2 have also been linked to various disease states including neurodevelopmental disorders and cancer.^{14–17} These proteins therefore potentially represent an important part of the protein homeostasis network but they remain largely uncharacterized.

In this study, we have developed both recombinant bacterial and mammalian cell systems for the expression and characterization of PCMTD1 in complex with Cullin-RING ligase (CRL) proteins. PCMTD1 and PCMTD2 are 79% identical, and it is likely that they have similar mechanisms. Our PCMTD1 constructs demonstrated consistent interactions between PCMTD1, Elongins B and C, and Cul5 across *in vitro* and in cell experiments (Figures 3 and 7). Importantly, C-terminally truncated PCMTD1 constructs did not associate with Elongins B and C, supporting the role of the C-terminally localized PCMTD1 SOCS box motif in Elongin recruitment (Figure 3). SOCS box-containing proteins perform a variety of regulatory functions within the cell, including SOCS1 ubiquitination of Jak2, Asb2 targeting of actin-binding filaments in leukemia cells, and VHL ubiquitination of HIF-1 α .^{45–47} It is clear from these few examples that the 80+ SOCS box proteins in the human genome play a significant role in maintaining cellular and human health, and thus an understanding of the putative PCMTD SOCS box protein mechanisms and targets is of utmost importance.

While substrates for the PCMTD proteins have yet to be identified, the discovery of the PCMTD1 association with CRL proteins in both recombinant and cellular contexts is an important step forward in our understanding of the SOCS box motif. Outside of the PCMTD proteins, the degenerate sequence between the BC-box and the Cul-box is typically 10 amino acids (Figure 1).¹⁰ In both PCMTD1 and PCMTD2, this linker region is comprised of ~90 residues (Figure 1). This study demonstrates that the extended linker does not disrupt

the association between PCMTD1, Elongins B and C, and Cul5 (Figures 3 and 7). Phylogenetic analysis of the PCMTD1 extended linker sequence across select metazoan phyla indicates a wide variety in sequence lengths ranging from 12 to 386 residues, with the average length being 145 residues, and the mode of these sequence lengths being 89 residues (Figure S2). When compared to previous PCMT1 crystal structures, the predicted structural models from AlphaFold demonstrate that the length of this linker could allow for a loop to wrap around the PCMTD1 globular core (PCMT1-homologous region) to extend over the presumed substrate binding site, where canonical L-isospartate binding motifs are localized, without disrupting the BC- or Cul-boxes (Figure S6).⁴⁸ If accurate, these models would indicate that the extended linker may play a role in substrate recruitment, binding, or release. Mutational studies, including the removal of this extended linker, could shed light on its role in future studies.

Purification of the full-length PCMTD1 alone proved difficult, while either coexpression with Elongins B and C or truncation of the PCMTD1 C-terminal domain allowed for robust purification of the PCMTD1–EloBC complex or PCMTD1^{1–231}, respectively (Figure 3). Expression and solubility tests revealed only modest increases in the expression of PCMTD1 in the presence of Elongins B and C (Figure 4A,B). Intriguingly, when PCMTD1 protein levels were monitored in induced cultures by immunoblot at various time points after the addition of a protein synthesis inhibitor, the results showed nearly complete loss of signal from the N-terminal His-tag of PCMTD1 after 120 min without Elongins (Figure 4C). In contrast, when PCMTD1 was coexpressed with Elongins, a strong signal from the N-terminal His-tag persisted throughout all time points. Loss of signal in the PCMTD1-alone samples may be explained by occlusion of the tag through misfolding, aggregation, or interacting partners or degradation of the PCMTD1 protein. While a faint band is seen near the molecular weight of PCMTD1 (42 kDa) in the Ponceau-stained blot, protein degradation cannot be ruled out, as the PCMTD1 construct also produces cleaved maltose binding protein after protein expression, which is approximately the same polypeptide molecular weight as PCMTD1 (42.5 kDa). The association between PCMTD1 and Elongins B and C within the *E. coli* expression system may prevent interaction with other partners that may occlude the His-tag from immunoblot detection or it may stabilize inherently disordered portions of the protein that may otherwise trigger unfolding or aggregation. The predicted AlphaFold model of PCMTD1 shows the lowest confidence metrics in the extended C-terminal linker region between the BC-box and the Cul-box, which may be an indicator of disorder within the protein structure (Figure S6). It is possible that Elongins B and C binding at the BC-box help order this region and prevent aggregation or degradation. Future biochemical and structural studies of PCMTD1 alone and in the presence of Elongins B and C may shed light on their stabilization of PCMTD1 protein levels.

PCMTD1 appears to associate better with Cul5 in our *in vitro* reconstitution experiments compared to either of our pulldown strategies (Figures 7 and 8). These results may be due to the sources from which PCMTD1 and Cul5 were derived in these experiments. For instance, recombinant PCMTD1 and Cul5 expressed in *E. coli* may not have their respective posttranslational modifications or other supplemen-

tal binding partners when found within their endogenous mammalian environments. However, these experiments still collectively suggest that a direct interaction occurs between PCMTD1 and Cul5.

In addition to demonstrating the interaction between PCMTD1 and CRL proteins, we have shown that PCMTD1 and PCMTD1^{1–231} associate with the methyltransferase cofactor AdoMet (Figure 5). Sequence comparisons, as well as structural comparisons between the PCMT1 structure and the AlphaFold predicted the PCMTD1 structure, reveal a few disruptive substitutions in the AdoMet binding domains, which corresponds with the observation that PCMTD1–EloBC is able to bind AdoMet (Figures 1 and 5). Interestingly, the C-terminally truncated PCMTD1 construct PCMTD1^{1–231} appears to exhibit decreased binding to AdoMet with respect to PCMTD1–EloBC (Figure 5). The PCMT1 crystal structure reveals that the C-terminus is approximately 8 Å away from the AdoMet binding site, while the predicted AlphaFold model of PCMTD1 shows the C-terminus extending from this point to form the SOCS box domain and further wrap around the PCMT1-homologous region (Figure S6).⁴⁹ It is possible that the removal of this extended C-terminus disrupts the PCMT1-homologous region of PCMTD1 adjacent to the AdoMet binding pocket, thereby lowering the affinity of the truncated PCMTD1 for the methyltransferase cofactor. There may also be an additional role for Elongins B and C in which the adaptor protein binding may allosterically enhance the association between PCMTD1 and AdoMet. Elongins B and C binding have been shown to induce conformational rearrangements of the substrate binding interface for ASB9, another Cullin-RING E3 ubiquitin ligase.⁴⁰

Surprisingly, despite evidence for AdoMet binding and conservation of the L-isospartyl-binding and AdoMet binding motifs within PCMTD1, no methyltransferase activity against L-isospartate-containing substrates or L-isospartate-rich tissue extracts was observed (Figure 6). The PCMTD1 construct is N-terminally 6xHis-tagged, and it is possible that the tag interferes with substrate binding; however, the recombinant PCMT1 construct used in this study is similarly N-terminally 6xHis-tagged and exhibits robust methyltransferase activity (Figure 6). Additionally, the isospartyl-binding site within the PCMT1 structure lies adjacent to the AdoMet binding pocket, and PCMTD1–EloBC is still able to bind AdoMet (Figures S6B and 5). While the radiolabeling methods used in this study are sufficient to detect as little as 1 fmol of methylation, further testing of different conditions and substrates may be necessary to detect PCMTD1 methyltransferase activity or demonstrate that the methyltransferase activity of this protein has been lost.

The cellular localization of the PCMTD proteins may affect their proposed physiological roles and enzymatic functions. We do note that these proteins contain a candidate nuclear localization signal—specifically 275-KRKRKR-280 in PCMTD1. Fluorescence microscopy of overexpressed PCMTD1 shows localization within the nucleus as well as the cytosol (Figure S7), consistent with Elongins B and C and Cul5 localization.^{50,51} This localization may be driven by its proposed basic nuclear localization signal (²⁷⁵KRKRKR²⁸⁰), but given the small size of the pGLAP2 PCMTD1 construct used here (~50 kDa), the observed nuclear localization may also be due to diffusion into the nucleus.⁵² Consistent with the idea of small proteins diffusing through the nuclear pore complex into the nucleus, our pGLAP2 EGFP (~30 kDa)

construct was also observed within the nucleus in our experiments (Figure S7).

This study adds to the limited knowledge available for the biochemical mechanisms of PCMTD1 and PCMTD2, and to the best of the authors' knowledge, only one previous study has included biochemical experiments with these proteins.⁴⁴ We have built on the previous study by investigating the interactions between PCMTD1 and CRL components, as well as its AdoMet binding and putative methyltransferase function. These results showed specific interactions with CRL components with the C-terminus of PCMTD1 and AdoMet binding within the N-terminus. These results suggest that the PCMTD proteins may be Cullin-RING E3 ubiquitin ligases that may recognize substrates that contain L-isoaspartate residues. Future work exploring the substrate specificity, ubiquitination activity, and structure of these proteins will reveal much about the mechanism and function of these proteins. This would represent a significant step forward in our understanding of RING ligase targeting, as recognition of L-isoaspartate in proteins would be the first example of an age-specific molecular switch. In this way, PCMTD1 and PCMTD2 may help maintain a functional proteome within the cell through the regular turnover of age-damaged proteins.

■ ASSOCIATED CONTENT

SI Supporting Information

The Supporting Information is available free of charge at <https://pubs.acs.org/doi/10.1021/acs.biochem.2c00130>.

Sequence variation across different human SOCS box-containing proteins (Figure S1); conserved regions between the PCMTD1 BC-box and Cul-box across metazoan phyla (Figure S2); multiple human isoforms of PCMTD result from alternative splicing (Figure S3); Elongins B and C copurifies with full-length PCMTD1 but not with truncated PCMTD1^{1–231} (Figure S4); Elongins B and C help stabilize the recombinant PCMTD1 replicate experiment (Figure S5); AlphaFold predicted structural model of human PCMTD1 (Figure S6); and microscopy of pGLAP2 EGFP and PCMTD1 constructs (Figure S7) (PDF)

Accession Codes

PCMT1: P22061-1, PCMTD1: Q96MG8-1, PCMTD2: Q9NV79-1, EloB: Q15370-1, EloC: Q15369-2, Cul5: Q93034, Rbx2: Q9WTZ1.

■ AUTHOR INFORMATION

Corresponding Author

Steven G. Clarke – *Department of Chemistry and Biochemistry and Molecular Biology Institute, University of California, Los Angeles, Los Angeles, California 90095, United States*; orcid.org/0000-0002-7303-6632;
Email: clarke@mbi.ucla.edu

Authors

Rebecca A. Warmack – *Department of Chemistry and Biochemistry and Molecular Biology Institute, University of California, Los Angeles, Los Angeles, California 90095, United States*; Present Address: Division of Chemistry and Chemical Engineering, California Institute of Technology, 1200 E. California Blvd., Pasadena, California 91125, United States

Eric Z. Pang – *Department of Chemistry and Biochemistry and Molecular Biology Institute, University of California, Los Angeles, Los Angeles, California 90095, United States*

Esther Peluso – *Department of Chemistry and Biochemistry and Molecular Biology Institute, University of California, Los Angeles, Los Angeles, California 90095, United States*

Jonathan D. Lowenson – *Department of Chemistry and Biochemistry and Molecular Biology Institute, University of California, Los Angeles, Los Angeles, California 90095, United States*

Joseph Y. Ong – *Department of Chemistry and Biochemistry and Molecular Biology Institute, University of California, Los Angeles, Los Angeles, California 90095, United States*

Jorge Z. Torres – *Department of Chemistry and Biochemistry and Molecular Biology Institute, University of California, Los Angeles, Los Angeles, California 90095, United States*;

orcid.org/0000-0002-2158-889X

Complete contact information is available at:

<https://pubs.acs.org/10.1021/acs.biochem.2c00130>

Author Contributions

[†]R.A.W. and E.Z.P. contributed equally to this work.

Funding

This work was supported by the National Science Foundation grant MCB-1714569 (to S.G.C.), the National Institutes of Health grant R35GM139539 (to J.Z.T), and by funds from the UCLA Academic Senate Faculty Research Program, the Life Extension Foundation, Inc., and the Elizabeth and Thomas Plott Chair in Gerontology of the UCLA Longevity Center (to S.G.C.). R.A.W. and J.Y.O. were supported by the National Institutes of Health Ruth L. Kirschstein National Research Service Award GM007185. E.Z.P. was supported by the NIH NIGMS-funded predoctoral fellowship (T32GM136614). J.Y.O. was supported by a National Science Foundation Graduate Research Fellowship DGE-1650604 and by a UCLA Whitcome Predoctoral Fellowship in Molecular Biology. The content is solely the responsibility of the authors and does not necessarily represent the official views of the National Institutes of Health.

Notes

The authors declare no competing financial interest.

This study was performed in accordance with animal use protocols approved by the UCLA Animal Research Committee (Protocol 1993-109-64). Mice were scheduled to be euthanized if they met any early removal criteria (kyphosis, lack of grooming behavior). However, this did not occur with any of the animals in our study.

Figures and tables were arranged in Adobe Illustrator. Signals from fluorographs were quantified by densitometry using ImageJ.⁵³

All data described in the manuscript are contained within the manuscript. Additional data are available upon request.

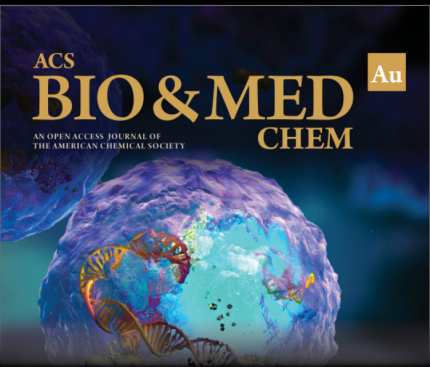
■ ACKNOWLEDGMENTS

The authors would like to acknowledge Dr. Mark Arbing and the UCLA DOE Protein Expression Core for aid in the design and synthesis of the plasmids used within this study. The authors would also like to thank Austin Gable, Georgiana Salant, Andrea Hadjikyriacou, Kennen MacKay, Calvin Lin, and Dylan Valencia for their contributions at the initial stages of this project.

REFERENCES

- (1) Santos, A. L.; Lindner, A. B. Protein Posttranslational Modifications: Roles in Aging and Age-Related Disease. *Oxid. Med. Cell. Longevity* **2017**, *2017*, No. 5716409.
- (2) Lourenço dos Santos, S.; Petropoulos, I.; Friguier, B. The Oxidized Protein Repair Enzymes Methionine Sulfoxide Reductases and Their Roles in Protecting Against Oxidative Stress, in Ageing and in Regulating Protein Function. *Antioxidants* **2018**, *7*, No. 191.
- (3) Van Schaftingen, E.; Collard, F.; Wiame, E.; Veiga-da-Cunha, M. Enzymatic Repair of Amadori Products. *Amino Acids* **2012**, *42*, 1143–1150.
- (4) Mishra, P. K. K.; Mahawar, M. PIMT-Mediated Protein Repair: Mechanism and Implications. *Biochemistry* **2019**, *84*, 453–463.
- (5) Chondrogianni, N.; Petropoulos, I.; Grimm, S.; Georgila, K.; Catalgol, B.; Friguier, B.; Grune, T.; Gonos, E. S. Protein damage, repair, and proteolysis. *Mol. Aspects Med.* **2014**, *35*, 1–71.
- (6) Yim, W. W.-Y.; Mizushima, N. Lysosome biology in autophagy. *Cell Discovery* **2020**, *6*, No. 6.
- (7) Berndsen, C. E.; Wolberger, C. New insights into ubiquitin E3 ligase mechanism. *Nat. Struct. Mol. Biol.* **2014**, *21*, 301–307.
- (8) Nguyen, H. C.; Wang, W.; Xiong, Y. Cullin-RING E3 Ubiquitin Ligases: Bridges to Destruction. In *Macromolecular Protein Complexes*. Subcellular Biochemistry; Harris, J. R.; Marles-Wright, J., Eds.; Springer International Publishing: Cham, 2017; Vol. 83, pp 323–347.
- (9) Deshaies, R. J.; Joazeiro, C. A. RING domain E3 ubiquitin ligases. *Annu. Rev. Biochem.* **2009**, *78*, 399–434.
- (10) Linossi, E. M.; Nicholson, S. E. The SOCS box-adapting proteins for ubiquitination and proteasomal degradation. *IUBMB Life* **2012**, *64*, 316–323.
- (11) Okumura, F.; Joo-Okumura, A.; Nakatsukasa, K.; Kamura, T. The role of cullin 5-containing ubiquitin ligases. *Cell Div.* **2016**, *11*, No. 1.
- (12) Lowenson, J. D.; Kim, E.; Young, S. G.; Clarke, S. Limited accumulation of damaged proteins in L-isoaspartyl (D-aspartyl) O-methyltransferase-deficient mice. *J. Biol. Chem.* **2001**, *276*, 20695–20702.
- (13) Gene [Internet]. National Library of Medicine (US), National Center for Biotechnology Information: Bethesda, MD, 2004. Available from <https://www.ncbi.nlm.nih.gov/gene/> [cited June 04, 2020].
- (14) Zarrei, M.; Burton, C. L.; Engchuan, W.; Young, E. J.; Higginbotham, E. J.; MacDonald, J. R.; Trost, B.; Chan, A. J. S.; Walker, S.; Lamoureux, S.; Heung, T.; Mojarad, B. A.; Kellam, B.; Paton, T.; Faheem, M.; Miron, K.; Lu, C.; Wang, T.; Samler, K.; Wang, X.; Costain, G.; Hoang, N.; Pellicchia, G.; Wei, J.; Patel, R. V.; Thiruvahindrapuram, B.; Roifman, M.; Merico, D.; Goodale, T.; Drmic, I.; Speevak, M.; Howe, J. L.; Yuen, R. K. C.; Buchanan, J. A.; Vorstman, J. A. S.; Marshall, C. R.; Wintle, R. F.; Rosenberg, D. R.; Hanna, G. L.; Woodbury-Smith, M.; Cytrynbaum, C.; Zwaigenbaum, L.; Elsabbagh, M.; Flanagan, J.; Fernandez, B. A.; Carter, M. T.; Szatmari, P.; Roberts, W.; Lerch, J.; Liu, X.; Nicolson, R.; Georgiades, S.; Weksberg, R.; Arnold, P. D.; Bassett, A. S.; Crosbie, J.; Schachar, R.; Stavropoulos, D. J.; Anagnostou, E.; Scherer, S. W. A large data resource of genomic copy number variation across neurodevelopmental disorders. *npj Genomic Med.* **2019**, *4*, No. 26.
- (15) Kroepfl, T.; Petek, E.; Schwarzbraun, T.; Kroisel, P. M.; Plecko, B. Mental retardation in a girl with a subtelomeric deletion on chromosome 20q and complete deletion of the myelin transcription factor 1 gene (MYT1). *Clin. Genet.* **2008**, *73*, 492–495.
- (16) Abere, B.; Samarina, N.; Gramolelli, S.; Rückert, J.; Gerold, G.; Pich, A.; Schulz, T. F. Kaposi's Sarcoma-Associated Herpesvirus Nonstructural Membrane Protein pK15 Recruits the Class II Phosphatidylinositol 3-Kinase PI3K-C2α To Activate Productive Viral Replication. *J. Virol.* **2018**, *92*, No. e00544-18.
- (17) Zimmer, A.; Amar-Farkash, S.; Danon, T.; Alon, U. Dynamic proteomics reveals bimodal protein dynamics of cancer cells in response to HSP90 inhibitor. *BMC Syst. Biol.* **2017**, *11*, No. 33.
- (18) Altschul, S. F.; Gish, W.; Miller, W.; Myers, E. W.; Lipman, D. J. Basic local alignment search tool. *J. Mol. Biol.* **1990**, *215*, 403–410.
- (19) Waterhouse, A. M.; Procter, J. B.; Martin, D. M. A.; Clamp, M.; Barton, G. J. Jalview Version 2-a multiple sequence alignment editor and analysis workbench. *Bioinformatics* **2009**, *25*, 1189–1191.
- (20) Notredame, C.; Higgins, D. G.; Heringa, J. T-Coffee: A novel method for fast and accurate multiple sequence alignment. *J. Mol. Biol.* **2000**, *302*, 205–217.
- (21) Kumar, S.; Stecher, G.; Li, M.; Nnyaz, C.; Tamura, K. MEGA X: Molecular Evolutionary Genetics Analysis across computing platforms. *Mol. Biol. Evol.* **2018**, *35*, 1547–1549.
- (22) Sievers, F.; Wilm, A.; Dineen, D.; Gibson, T. J.; Karplus, K.; Li, W.; Lopez, R.; McWilliam, H.; Remmert, M.; Söding, J.; Thompson, J. D.; Higgins, D. G. Fast, scalable generation of high-quality protein multiple sequence alignments using Clustal Omega. *Mol. Syst. Biol.* **2011**, *7*, 537–539.
- (23) Thorne, C. J. R. *Techniques in Protein and Enzyme Biochemistry*, Elsevier/North-Holland, 1978; pp 2–18.
- (24) Patananan, A. N.; Capri, J.; Whitelegge, J. P.; Clarke, S. G. Non-repair Pathways for Minimizing Protein Isoaspartyl Damage in the Yeast *Saccharomyces cerevisiae*. *J. Biol. Chem.* **2014**, *289*, 16936–16953.
- (25) MacKay, K. B.; Lowenson, J. D.; Clarke, S. G. Wortmannin Reduces Insulin Signaling and Death in Seizure-Prone Pcnt1-1/1 Mice. *PLoS One* **2012**, *7*, No. e46719.
- (26) Katz, J. E.; Dlakić, M.; Clarke, S. Automated identification of putative methyltransferases from genomic open reading frames. *Mol. Cell. Proteomics* **2003**, *2*, 525–540.
- (27) Griffith, S. C.; Sawaya, M. R.; Boutz, D. R.; Thapar, N.; Katz, J. E.; Clarke, S.; Yeates, T. O. Crystal structure of a protein repair methyltransferase from *Pyrococcus furiosus* with its L-isoaspartyl peptide substrate 1 Edited by I. A. Wilson. *J. Mol. Biol.* **2001**, *313*, 1103–1116.
- (28) Kamura, T.; Sato, S.; Haque, D.; Liu, L.; Kaelin, W. G.; Conaway, R. C.; Conaway, J. W. The Elongin BC complex interacts with the conserved SOCS-box motif present in members of the SOCS, ras, WD-40 repeat, and ankyrin repeat families. *Genes Dev.* **1998**, *12*, 3872–3881.
- (29) Babon, J. J.; Sabo, J. K.; Soetopo, A.; Yao, S.; Bailey, M. F.; Zhang, J. G.; Nicola, N. A.; Norton, R. S. The SOCS box domain of SOCS3: structure and interaction with the elonginBC-cullin5 ubiquitin ligase. *J. Mol. Biol.* **2008**, *381*, 928–940.
- (30) Stebbins, C. E.; Kaelin, W. G.; Pavletich, N. P. Structure of the VHL-ElonginC-ElonginB complex: implications for VHL tumor suppressor function. *Science* **1999**, *284*, 455–461.
- (31) Lu, S.; Wang, J.; Chitsaz, F.; Derbyshire, M. K.; Geer, R. C.; Gonzales, N. R.; Gwadz, M.; Hurwitz, D. L.; Marchler, G. H.; Song, J. S.; Thanki, N.; Yamashita, R. A.; Yang, M.; Zhang, D.; Zheng, C.; Lanczycki, C. J.; Marchler-Bauer, A. CDD/SPARCLE: the conserved domain database in 2020. *Nucleic Acids Res.* **2020**, *48*, D265–D268.
- (32) Liongue, C.; Taznin, T.; Ward, A. C. Signaling via the CytoR/JAK/STAT/SOCS pathway: Emergence during evolution. *Mol. Immunol.* **2016**, *71*, 166–175.
- (33) Punta, M.; Coghill, P. C.; Eberhardt, R. Y.; Mistry, J.; Tate, J.; Boursnell, C.; Pang, N.; Forslund, K.; Ceric, G.; Clements, J.; Heger, A.; Holm, L.; Sonnhammer, E. L.; Eddy, S. R.; Bateman, A.; Finn, R. D. The Pfam protein families database. *Nucleic Acids Res.* **2012**, *40*, D290–D301.
- (34) The UniProt Consortium. UniProt: a worldwide hub of protein knowledge. *Nucleic Acids Res.* **2019**, *47*, D506–D515.
- (35) Ota, T.; Suzuki, Y.; Nishikawa, T.; Otsuki, T.; Sugiyama, T.; Irie, R.; Wakamatsu, A.; Hayashi, K.; Sato, H.; Nagai, K.; Kimura, K.; Makita, H.; Sekine, M.; Obayashi, M.; Nishi, T.; Shibahara, T.; Tanaka, T.; Ishii, S.; Yamamoto, J.; Saito, K.; Kawai, Y.; Isono, Y.; Nakamura, Y.; Nagahari, K.; Murakami, K.; Yasuda, T.; Iwayanagi, T.; Wagatsuma, M.; Shiratori, A.; Sudo, H.; Hosoiri, T.; Kaku, Y.; Kodaira, H.; Kondo, H.; Sugawara, M.; Takahashi, M.; Kanda, K.; Yokoi, T.; Furuya, T.; Kikkawa, E.; Omura, Y.; Abe, K.; Kamihara, K.; Katsuta, N.; Sato, K.; Tanikawa, M.; Yamazaki, M.; Ninomiya, K.; Ishibashi, T.; Yamashita, H.; Murakawa, K.; Fujimori, K.; Tanai, H.; Kimata, M.; Watanabe, M.; Hiraoka, S.; Chiba, Y.; Ishida, S.; Ono, Y.;

- Takiguchi, S.; Watanabe, S.; Yosida, M.; Hotuta, T.; Kusano, J.; Kanehori, K.; Takahashi-Fujii, A.; Hara, H.; Tanase, T.; Nomura, Y.; Togiya, S.; Komai, F.; Hara, R.; Takeuchi, K.; Arita, M.; Imose, N.; Musashino, K.; Yuuki, H.; Oshima, A.; Sasaki, N.; Aotsuka, S.; Yoshikawa, Y.; Matsunawa, H.; Ichihara, T.; Shiohata, N.; Sano, S.; Moriya, S.; Momiyama, H.; Satoh, N.; Takami, S.; Terashima, Y.; Suzuki, O.; Nakagawa, S.; Senoh, A.; Mizoguchi, H.; Goto, Y.; Shimizu, F.; Wakebe, H.; Hishigaki, H.; Watanabe, T.; Sugiyama, A.; Takemoto, M.; Kawakami, B.; Yamazaki, M.; Watanabe, K.; Kumagai, A.; Itakura, S.; Fukuzumi, Y.; Fujimori, Y.; Komiyama, M.; Tashiro, H.; Tanigami, A.; Fujiwara, T.; Ono, T.; Yamada, K.; Fujii, Y.; Ozaki, K.; Hirao, M.; Ohmori, Y.; Kawabata, A.; Hikiji, T.; Kobatake, N.; Inagaki, H.; Ikema, Y.; Okamoto, S.; Okitani, R.; Kawakami, T.; Noguchi, S.; Itoh, T.; Shigeta, K.; Senba, T.; Matsumura, K.; Nakajima, Y.; Mizuno, T.; Morinaga, M.; Sasaki, M.; Togashi, T.; Oyama, M.; Hata, H.; Watanabe, M.; Komatsu, T.; Mizushima-Sugano, J.; Satoh, T.; Shirai, Y.; Takahashi, Y.; Nakagawa, K.; Okumura, K.; Nagase, T.; Nomura, N.; Kikuchi, H.; Masuho, Y.; Yamashita, R.; Nakai, K.; Yada, T.; Nakamura, Y.; Ohara, O.; Isogai, T.; Sugano, S. Complete sequencing and characterization of 21,243 full-length human cDNAs. *Nat. Genet.* **2004**, *36*, 40–45.
- (36) Bechtel, S.; Rosenfelder, H.; Duda, A.; Schmidt, C.; Ernst, U.; Wellenreuther, R.; Mehrle, A.; Schuster, C.; Bahr, A.; Blöcker, H.; Heubner, D.; Hoerlein, A.; Michel, G.; Wedler, H.; Köhler, K.; Ottenwälder, B.; Poustka, A.; Wiemann, S.; Schupp, I. The full-ORF clone resource of the German cDNA Consortium. *BMC Genomics* **2007**, *8*, No. 399.
- (37) The MGC Project Team. The status, quality, and expansion of the NIH full-length cDNA project: the Mammalian Gene Collection (MGC). *Genome Res.* **2004**, *14*, 2121–2127.
- (38) Zheng, N.; Schulman, B. A.; Song, L.; Miller, J. J.; Jeffrey, P. D.; Wang, P.; Chu, C.; Koepp, D. M.; Elledge, S. J.; Pagano, M.; Conaway, R. C.; Conaway, J. W.; Harper, J. W.; Pavletich, N. P. Structure of the Cul1-Rbx1-Skp1-F boxSkp2 SCF ubiquitin ligase complex. *Nature* **2002**, *416*, 703–709.
- (39) Babon, J. J.; Sabo, J. K.; Soetopo, A.; Yao, S.; Bailey, M. F.; Zhang, J. G.; Nicola, N. A.; Norton, R. S. The SOCS3 box domain of SOCS3: structure and interaction with the elonginBC-cullin5 ubiquitin ligase. *J. Mol. Biol.* **2008**, *381*, 928–940.
- (40) Lumpkin, R. J.; Baker, R. W.; Leschziner, A. E.; Komives, E. A. Structure and dynamics of the ASB9 CUL-RING E3 Ligase. *Nat Commun.* **2020**, *11*, No. 2866.
- (41) Lowenson, J. D.; Clarke, S. Structural elements affecting the recognition of L-isoaspartyl residues by the L-isoaspartyl/D-aspartyl protein methyltransferase: implications for the repair hypothesis. *J. Biol. Chem.* **1991**, *266*, 19396–19406.
- (42) Pey, A. L. *Protein Homeostasis and Disease*, Academic Press, 2020; Chapter 2.
- (43) Calamini, B.; Morimoto, R. I. Protein Homeostasis as a Therapeutic Target for Diseases of Protein Conformation. *Curr. Top. Med. Chem.* **2013**, *12*, 2623–2640.
- (44) Mahrouf, N.; Redwine, W. B.; Florens, L.; Swanson, S. K.; Martin-Brown, S.; Bradford, W. D.; Staehling-Hampton, K.; Washburn, M. P.; Conaway, R. C.; Conaway, J. W. Characterization of Cullin-box sequences that direct recruitment of Cul2-Rbx1 and Cul5-Rbx2 modules to Elongin BC-based ubiquitin ligases. *J. Biol. Chem.* **2008**, *283*, 8005–8013.
- (45) Razinia, Z.; Baldassarre, M.; Bouaouina, M.; Lamsoul, I.; Lutz, P. G.; Calderwood, D. A. The E3 ubiquitin ligase specificity subunit ASB2 α targets flamins for proteasomal degradation by interacting with the filamin actin-binding domain. *J. Cell Sci.* **2011**, *124*, 2631–2641.
- (46) Ungureanu, D.; Saharinen, P.; Junttila, I.; Hilton, D. J.; Silvennoinen, O. Regulation of Jak2 through the ubiquitin-proteasome pathway involves phosphorylation of Jak2 on Y1007 and interaction with SOCS-1. *Mol. Cell. Biol.* **2002**, *22*, 3316–3326.
- (47) Iwai, K.; Yamanaka, K.; Kamura, T.; Minato, N.; Conaway, R. C.; Conaway, J. W.; Klausner, R. D.; Pause, A. Identification of the von Hippel–Lindau tumor-suppressor protein as part of an active E3 ubiquitin ligase complex. *Proc. Natl. Acad. Sci. U.S.A.* **1999**, *96*, 12436–12441.
- (48) Jumper, J.; Evans, R.; Pritzel, A.; Green, T.; Figurnov, M.; Ronneberger, O.; Tunyasuvunakool, K.; Bates, R.; Zidek, A.; Potapenko, A.; Bridgland, A.; Meyer, C.; Kohli, S. A. A.; Ballard, A. J.; Cowie, A.; Romera-Paredes, B.; Nikolov, S.; Jain, R.; Adler, J.; Back, T.; Petersen, S.; Reiman, D.; Clancy, E.; Zielinski, M.; Steinegger, M.; Pacholska, M.; Berghammer, T.; Bodenstein, S.; Silver, D.; Vinyals, O.; Senior, A. W.; Kavukcuoglu, K.; Kohli, P.; Hassabis, D. Highly accurate protein structure prediction with AlphaFold. *Nature* **2021**, *596*, 583–589.
- (49) Ryttersgaard, C.; Griffith, S. C.; Sawaya, M. R.; MacLaren, D. C.; Clarke, S.; Yeates, T. O. Crystal structure of human L-isoaspartyl methyltransferase. *J. Biol. Chem.* **2002**, *277*, 10642–10646.
- (50) Zhang, Z.; Huang, Q.; Wang, Z.; Zou, J.; Yu, Z.; Strauss, J. F., III; Zhang, Z. Elongin B is a binding partner of the male germ cell nuclear speckle protein sperm-associated antigen 16S (SPAG16S) and is regulated post-transcriptionally in the testis. *Reprod. Fertil. Dev.* **2019**, *31*, 962.
- (51) Weems, J. C.; Slaughter, B. D.; Unruh, J. R.; Hall, S. M.; McLaird, M. B.; Gilmore, J. M.; Washburn, M. P.; Florens, L.; Yasukawa, T.; Aso, T.; Conaway, J. W.; Conaway, R. C. Assembly of the Elongin A Ubiquitin Ligase Is Regulated by Genotoxic and Other Stresses. *J. Biol. Chem.* **2015**, *290*, 15030–15041.
- (52) Timney, B. L.; Raveh, B.; Mironska, R.; Trivedi, J. M.; Kim, S. J.; Russel, D.; Wentz, S. R.; Sali, A.; Rout, M. P. Simple rules for passive diffusion through the nuclear pore complex. *J. Cell Biol.* **2016**, *215*, 57–76.
- (53) Schneider, C. A.; Rasband, W. S.; Eliceiri, K. W. NIH Image to ImageJ: 25 years of image analysis. *Nat. Methods* **2012**, *9*, 671–675.



ACS
BIO & MED Au
CHEM
AN OPEN ACCESS JOURNAL OF
THE AMERICAN CHEMICAL SOCIETY

Editor-in-Chief: **Prof. Shelley D. Minter**, University of Utah, USA

Deputy Editor
Prof. Squire J. Booker
Pennsylvania State University, USA

Open for Submissions 

pubs.acs.org/biomedchemau  ACS Publications
Most Trusted. Most Cited. Most Read.

Supporting Information

The human protein-L-isoaspartate *O*-methyltransferase domain-containing protein 1 (PCMTD1) associates with Cullin-RING ligase proteins

Rebecca A. Warmack^{a,b}, Eric Z. Pang^a, Esther Peluso, Jonathan D. Lowenson, Joseph Y. Ong, Jorge Z. Torres, Steven G. Clarke^{*}

^aThese authors contributed equally to this work.

Department of Chemistry and Biochemistry and the Molecular Biology Institute, University of California, Los Angeles, 607 Charles E. Young Drive East, Los Angeles, CA 90095, USA

^bPresent Address: Division of Chemistry and Chemical Engineering, California Institute of Technology, 1200 E. California Blvd., CA 91125, USA

^{*}To whom correspondence should be addressed: UCLA Department of Chemistry and Biochemistry, 607 Charles E. Young Dr. E., Los Angeles, California 90095. E-mail: clarke@mbi.ucla.edu

Materials included:

Figures S1-S7

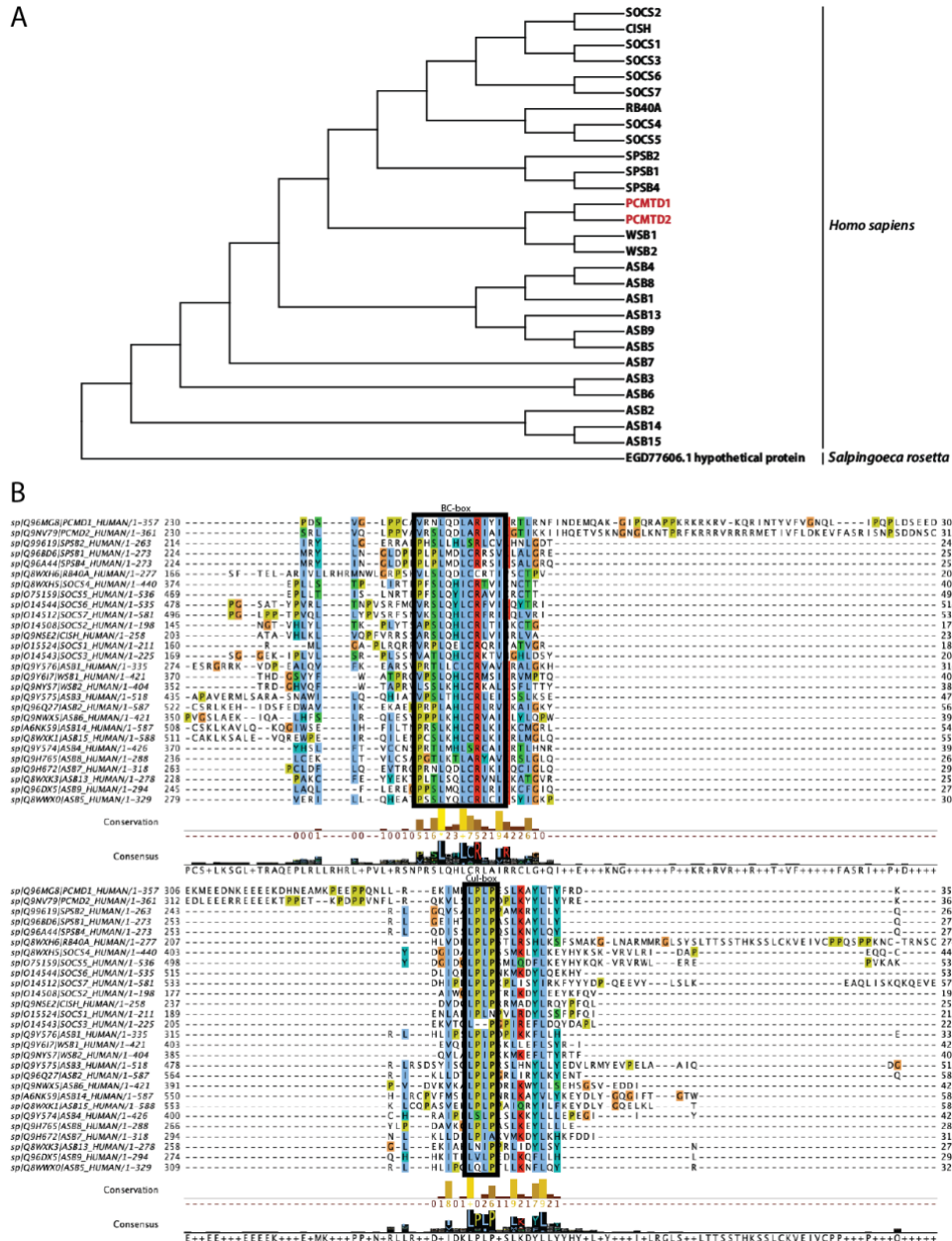
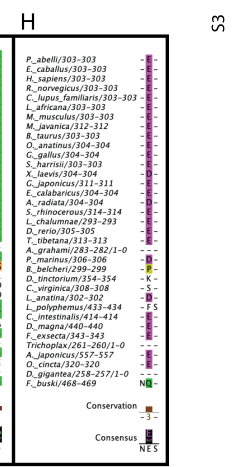
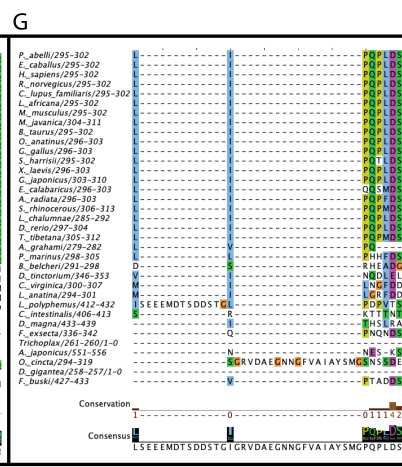
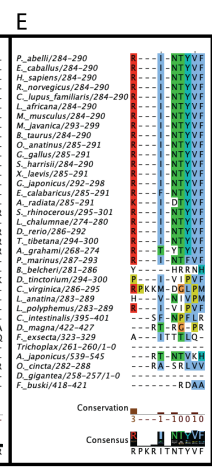
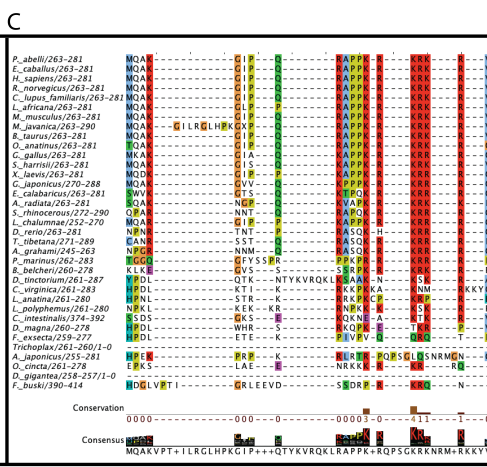
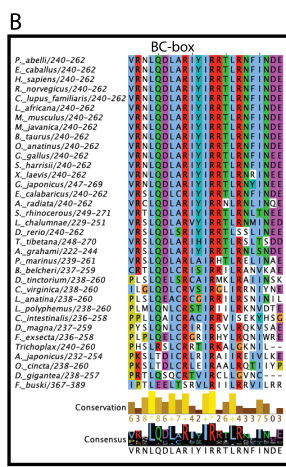
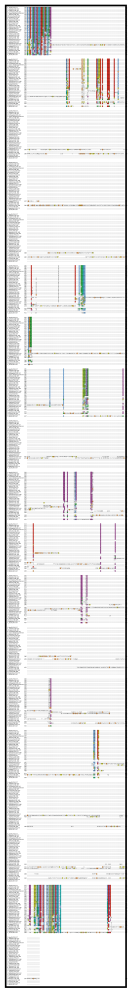


Figure S1. Sequence variation across different human SOCS box-containing proteins. **A.** A maximum likelihood tree comparing full sequences of human PCMTD proteins to full sequences of human SOCS box-containing proteins. The sequence of EGD77606.1 is a putative SOCS box protein from the choanoflagellate *S. rosetta* and acts as an outgroup to the human species. Accession numbers are indicated in bars, followed by protein name, and amino acid length of sequence. **B.** Sequences of the PCMTDs were aligned with SOCS box-containing proteins from the suppressor of cytokine signaling proteins (SOCS1-7), WD repeat and SOCS box-containing proteins (WSB1-2), Cytokine-inducible SH2-containing protein (CISH), Ras-related protein (RB40A), SPRY domain-containing SOCS box proteins (SPSB1-2, 4), and the Ankyrin repeat and SOCS box proteins. Only partial C-termini of the proteins are displayed to highlight the BC-box and the Cul-box (outlined). Unconserved residues are white. For conserved residues the color scheme is as follows: hydrophobic (blue), positive charge (red), negative charge (magenta), polar (green), cysteine (pink), glycine (orange), proline (yellow), aromatic (cyan).

A



S

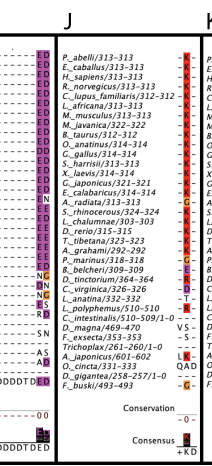
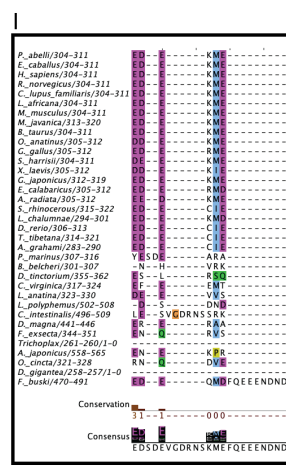


Figure S2. Conserved regions between the PCMTD1 BC-box and Cul-box across metazoan phyla. A protein BLAST search was performed against PCMTD1 isoform 1. Species were selected from each phylum that was identified and a multiple sequence alignment was performed. **A.** A T-Coffee multiple sequence alignment of PCMTD1 sequences was generated. **B-O.** Panels represent consecutive regions between the BC-box and the Cul-box of isoform 1 that have more than one or more conserved residues. Unconserved residues are white. For conserved residues the color scheme is as follows: hydrophobic (blue), positive charge (red), negative charge (magenta), polar (green), cysteine (pink), glycine (orange), proline (yellow), aromatic (cyan).

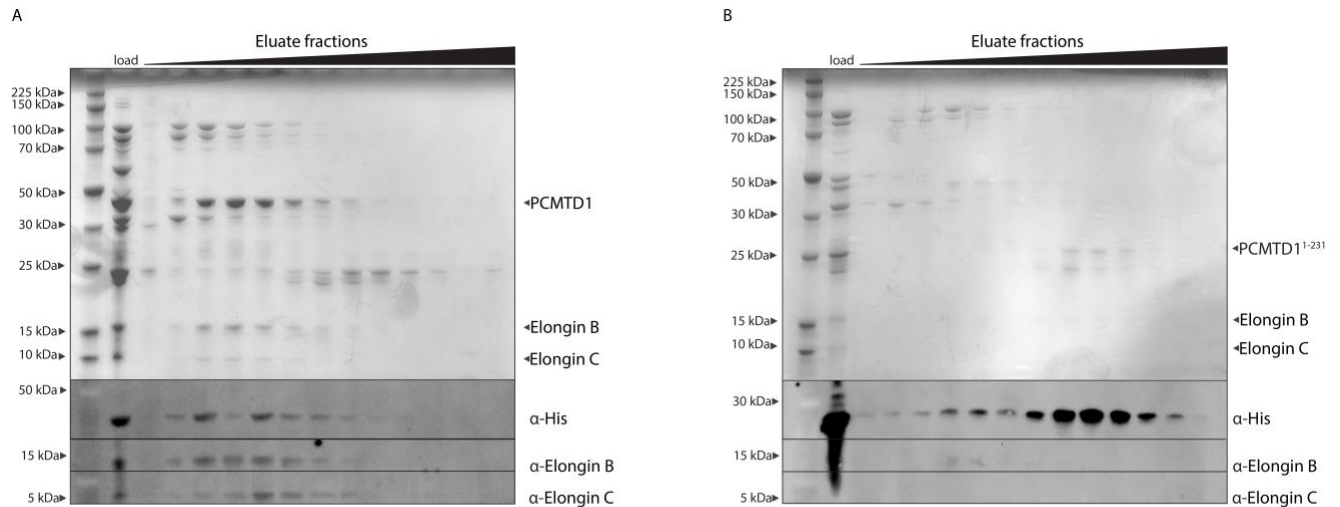


Figure S4. Elongins B and C co-purifies with full-length PCMTD1 but not with truncated PCMTD1¹⁻²³¹. **A.** Following His-tag purification of a full-length N-terminal His-tagged PCMTD1 construct co-expressed with EloB and EloC, eluates containing protein were pooled and concentrated for size exclusion chromatography. Here, Elongins B and C were found to co-elute with the full-length PCMTD1 protein. The top gel represents a Coomassie stain of the size exclusion fractions and the immunoblots below represent immunostaining of a blot of a gel that was loaded equivalently. Load lane represents samples pooled after His-tag purification of recombinantly co-expressed 6xHis-PCMTD1 and Elongins B and C used for further purification via gel filtration. **B.** Following His-tag purification of a truncated N-terminal His-tagged PCMTD1¹⁻²³¹ construct co-expressed with Elongins B and C, fractions were pooled and concentrated. Size exclusion chromatography indicated that the N-terminal His-tagged PCMTD1¹⁻²³¹ does not co-elute with Elongins B and C. Load lane represents samples pooled after His-tag purification of recombinantly co-expressed 6xHis-PCMTD1¹⁻²³¹ and Elongins B and C used for further purification via gel filtration.

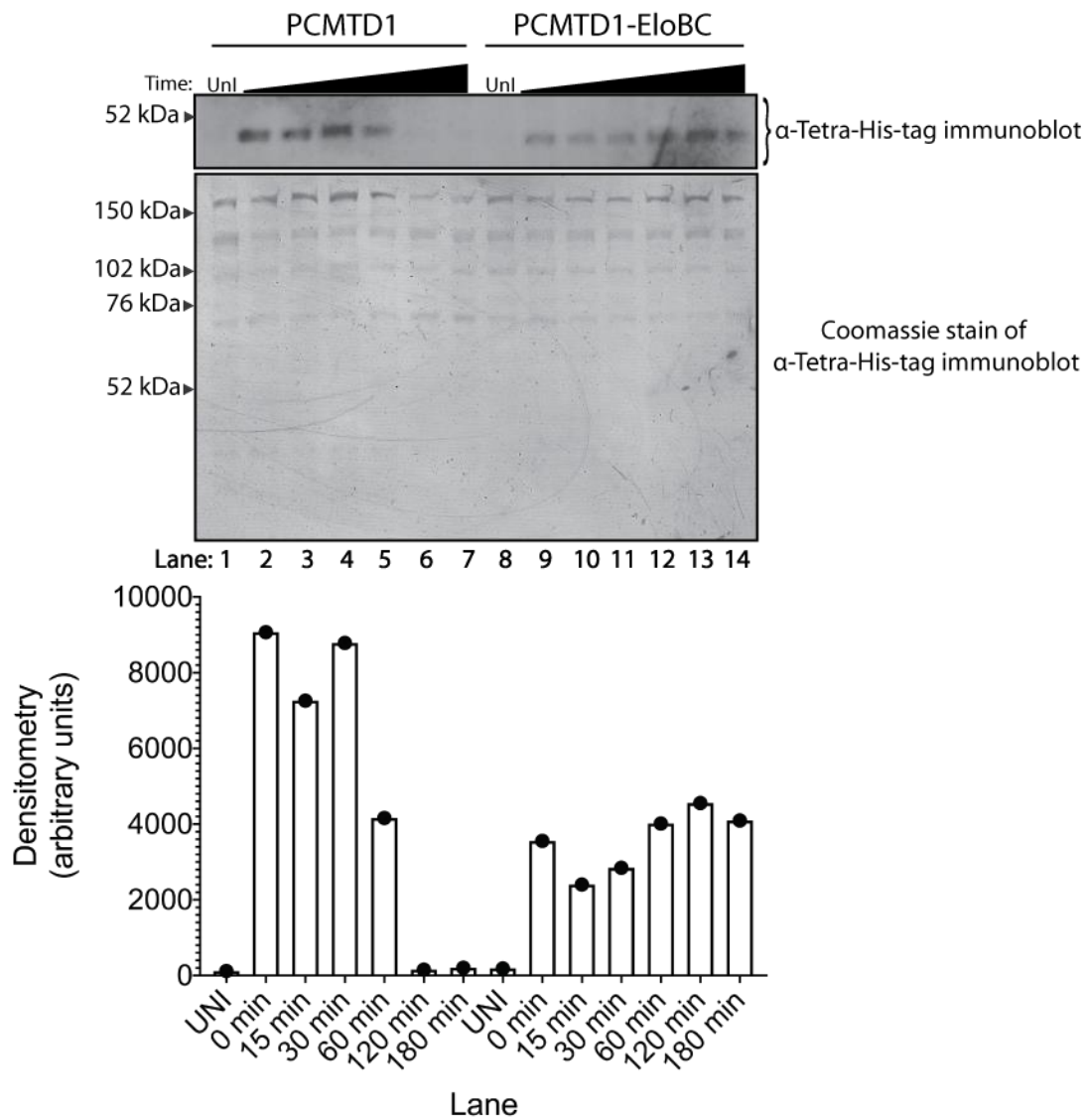


Figure S5. Elongins B and C help stabilize recombinant PCMTD1 replicate experiment. *E. coli* cells expressing PCMTD1 alone (lanes 1-7) or PCMTD1 with Elongins B and C (lanes 8-14) were treated with 25 $\mu\text{g}/\text{mL}$ tetracycline as described in the Methods section. Lanes 1 and 8 represent uninduced cultures. Succeeding lanes show increasing time points after induced strains were treated with tetracycline. Lower panel represents densitometric quantification of the PCMTD1 band detected by anti-Tetra-His-tag antibody.

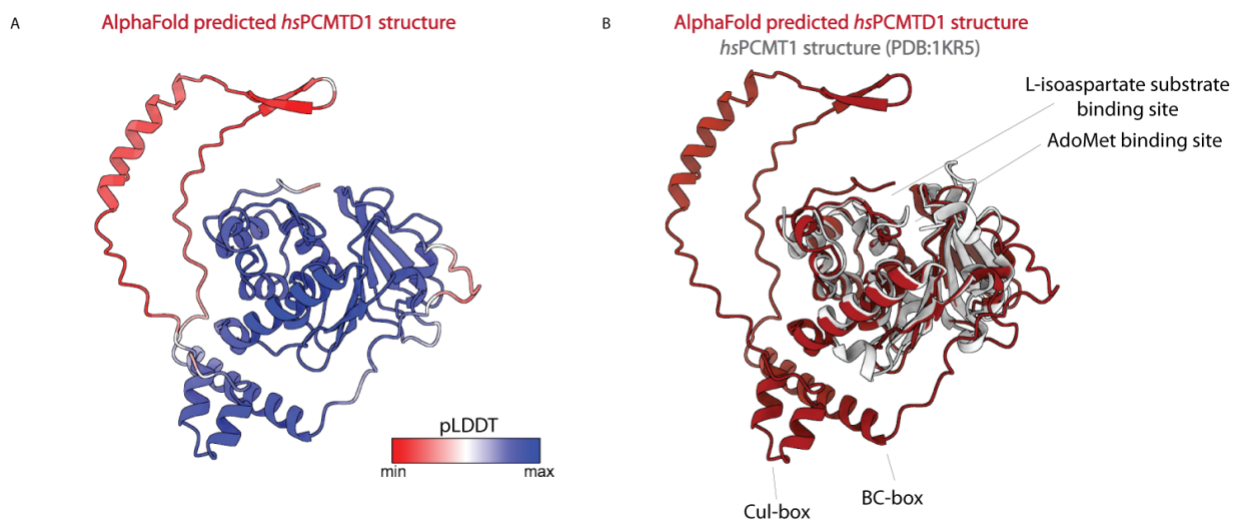


Figure S6. AlphaFold predicted structural model of human PCMTD1. **A.** Predicted structural model of human PCMTD1 from the AlphaFold Protein Structure Database (48). Backbone is colored by the per-residue confidence metric, predicted local distance difference test (pLDDT) with areas of higher confidence in blue and areas of lower confidence in red. **B.** Predicted structural model of human PCMTD1 overlaid with the human PCMTD1 crystal structure (PDB 1KR5; ref. 49).

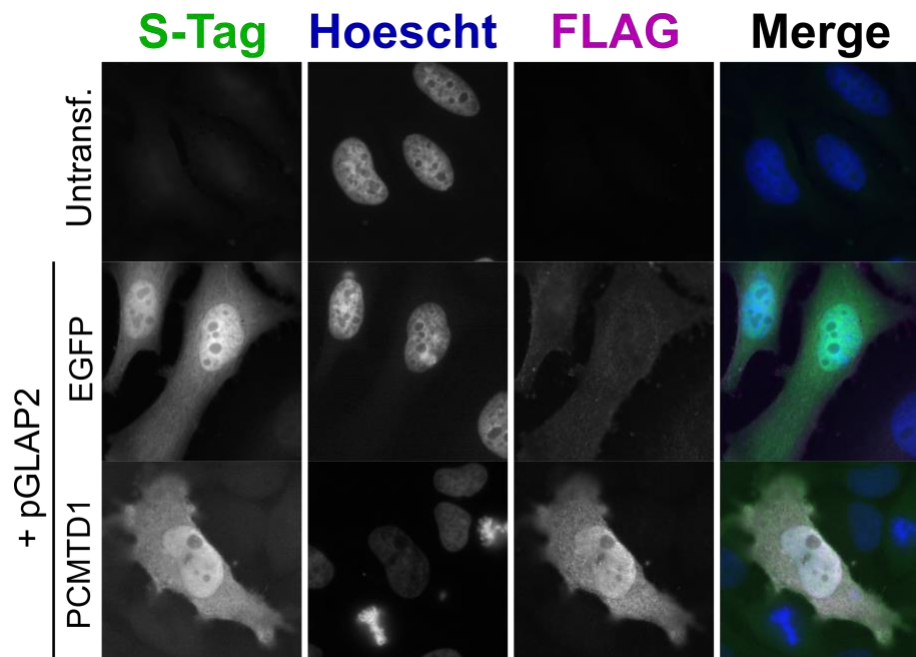


Figure S7. Microscopy of pGLAP2 EGFP and PCMTD1 constructs. 500 ng of pGLAP2 EGFP and PCMTD1 were transiently transfected into HeLa cells with 1.5 μ L of Fugene 6. 48 hours after transfection, the cells were fixed with 4% PFA in PBS for 15 minutes at 37° C, permeabilized with 0.2% Triton X-100 in PBS for 1 minute, and stained with Hoescht 33342 (1 μ g/mL) and antibodies (S-Tag: GeneTex, GTX19321, used at 1:100; FLAG: Cell Signaling Technology, #14793, used at 1:200; secondary antibodies from Jackson Immuno, used at 1:500). Images were captured with a Leica DMI6000 microscope (Leica DFC360 FX Camera; 63 \times /1.40-0.60 NA oil objective; Leica AF6000 software). Each image is 71.67 microns square. Untransf., untransfected HeLa cells.